Chapter Six

Ethane, fluoroethane and hexafluoroethane

Introduction

The study of the electric and magnetic properties of ethane has a long history and continual refinement of the numerical values has occurred, especially during the last fifteen years. In this chapter, the depolarization ratio and mean polarizability of ethane are reported, in an attempt to remove any remaining doubt about these values. Depolarization ratios and mean polarizabilities are also reported for fluoroethane and hexafluoroethane, to study the effect of fluorine substitution into ethane. The results for fluoroethane complement a study of the other haloethanes by Ritchie *et al.* [1]. Ab initio calculations of the polarizabilities are included for hexafluoroethane.

Experimental details

Ethane (> 99.0%) and hexafluoroethane (> 99.6%) were obtained from Matheson Gas Products; fluoroethane (> 99%) was obtained from Pfaltz and Bauer, Inc. All three gases were used without further purification. The ratios were recorded with Version 2 of the apparatus at 25 °C and ≈ 100 kPa, with inclusion and exclusion of the vibrational Raman lines. For ethane, fluoroethane and hexafluoroethane, typical polarized and depolarized count rates were 57 000 and 120 cps, 48 590 and 133 cps, and 71 900 and 37 cps, with background counts of 20 and 6 cps, 18 and 4 cps, and 24 and 6 cps, respectively. Integration times of 100 s for the polarized component and 200 s for the depolarized component were used for fluoroethane. Integration times were lengthened by

a factor of five for ethane and hexafluoroethane to reduce the uncertainties. The depolarization ratios are given in Table 6.1.

Values of the mean polarizability were determined for both ethane and hexafluoroethane with exclusion of the vibrational Raman lines. Three values were determined for fluoroethane, two of which excluded the vibrational Raman lines. Density second virial coefficients used in the calculations were obtained from the literature [2,3]. A summary of the depolarization ratios, mean polarizabilities and polarizability anisotropies is given in Table 6.2.

Table 6.1 Depolarization ratios for ethane, fluoroethane and hexafluoroethane.

$100\rho_0$		
ethane	fluoroethane	hexafluoroethane
0.199 ± 0.003	0.272 ± 0.003	0.043 ± 0.003
0.199 ± 0.003	0.274 ± 0.003	0.042 ± 0.002
0.198 ± 0.003	0.273 ± 0.002	0.044 ± 0.002
0.200 ± 0.003	0.265 ± 0.002	0.043 ± 0.002
0.198 ± 0.003	0.266 ± 0.002	0.030 ± 0.003[a]
0.159 ± 0.003[a]	0.227 ± 0.003[a]	0.029 ± 0.003[a]
0.160 ± 0.003[a]	0.228 ± 0.003[a]	0.026 ± 0.003[a]
0.157 ± 0.003[a]	0.225 ± 0.003[a]	0.029 ± 0.003[a]
0.158 ± 0.003[a]	0.229 ± 0.003[a]	
	0.227 ± 0.003[a]	

[a] Vibrational Raman lines excluded.

Table 6.2 Depolarization ratios, mean polarizabilities and polarizability anisotropies of ethane, fluoroethane and hexafluoroethane.

Molecule	λ(nm)	$100\rho_0$	α	$\Delta\alpha$	Reference
C_2H_6	632.8	0.199 ± 0.001			Present work
	632.8	0.159 ± 0.001[a]	5.00 ± 0.05[a]	0.77 ± 0.01	Present work
	632.8		4.97		[4]
	632.8		5.01		[5]
	632.8		4.97		[6]
	632.8		5.00		[7]
	632.8		4.958		[8]
	632.8		4.966		[9]
C_2H_5F	632.8	0.270 ± 0.005	5.07 ± 0.02		Present work
	632.8	0.227 ± 0.002[a]	5.02 ± 0.02[a]	0.93 ± 0.01[e]	Present work
	632.8		5.03 ± 0.02[a]		Present work
	589		4.93		[10]
	∞		5.52		[11]
C_2F_6	632.8	0.043 ± 0.001			Present work
	632.8	0.029 ± 0.002[a]	5.66 ± 0.03[a]	−0.35 ± 0.01[d]	Present work
	632.8		5.37 ± 0.15[b]		[12]
	514.5	0.008[a]	6.71	−0.23[d]	[13]
	∞		6.3[c]		[11]

[a] Vibrational Raman lines excluded.

[b] An uncertainty of ± 3% was assumed.

[c] This value contains a correction for the vibrational polarizability [14].

[d] The sign of $\Delta\alpha$ has been assumed on the basis of ab initio calculations.

[e] For fluoroethane, $\Delta\alpha$ is given as $|3\alpha\kappa|$.

Discussion

From Table 6.2, the present mean polarizability for ethane of α = 5.00 is in excellent agreement with the value of α = 5.01 derived by Bogaard *et al.* [5] from gas-phase refractive indices, and a value of α = 5.00 from interferometric measurements of refractive indices reported by Kerl and Haüssler [7]. Independent interferometric measurements reported by Hohm [9] and Achtermann and Magnus [8] have refined this value to approximately 4.97, and it is supported by studies of dipole oscillator-strength distributions reported by Meath and co-workers [6]. A value of α = 5.00 ± 0.05 is used in the present analysis.

There are few literature values of the mean polarizability for fluoroethane and hexafluoroethane. For fluoroethane, a static mean polarizability obtained from measurements of the relative permittivity [11] which is uncorrected for the vibrational polarizability, and a mean polarizability for 589 nm obtained from liquid-phase refractive indices [10] are the only two literature values available, and these do not agree. It is surprising that, of the three mean polarizabilities determined in the present research, the value which includes the vibrational Raman lines is higher than the values which exclude the vibrational Raman lines. The method used here to determine the mean polarizability involves measuring the polarized counts as a function of number density, and taking the ratio of the gradients for use in equation 1.25. Therefore, excluding the vibrational Raman lines should reduce the counts but not alter the gradients. A mean polarizability of α = 5.02 ± 0.05 was used in the present analysis.

For hexafluoroethane, a static mean polarizability obtained from measurements of the relative permittivity [11] with a vibrational polarizability correction of α_{vib} = 1.3 [14], is too high compared to the present value. A mean polarizability of α = 6.71 is quoted by Haverkort *et al.* [13], but this is certainly an overestimate. Another value of α = 5.37 reported by Bulanin *et al.* [12] from gas-phase refractive indices is in much better agreement, although lower than the present result by approximately 5%. The MP2 calculation of the mean polarizability given in the next section, with a 5% scaling factor [15], tends to support the value reported by Bulanin *et al.*, but this is a tenuous argument

dependent on the accuracy of the calculations. The value reported by Bulanin *et al.* was used in the derivation of the polarizability components for hexafluoroethane.

This is the first reported study of the depolarization ratio for fluoroethane. For hexafluoroethane, a value of $100\rho_n = 0.008$ has been reported by Haverkort *et al.* [13] which differs significantly (smaller by a factor of four) from the present ratio. The depolarization ratios for ethane and nitrogen reported by Haverkort *et al.* are in reasonable agreement with the ratios obtained in the present work (the depolarization ratio for nitrogen is given in Chapter 10). Overall, the data reported by Haverkort *et al.* appear to be very reliable, and the large difference between the present depolarization ratio and the value reported by Haverkort *et al.* cannot be explained. It is unlikely that dispersion in the ratios is the cause of the discrepancy. Haverkort *et al.* do not report an uncertainty for the depolarization ratio, but the instrumental depolarization was found to be 5×10^{-5}, which is of the same order of magnitude as the depolarization ratio. An instrumental depolarization could not be determined for the present apparatus (Chapter 10) and therefore the ratios are not corrected. The depolarization ratio of hexafluoroethane is extremely small and may be approaching the limit of detection of the present apparatus. Combining the depolarization ratio reported by Haverkort *et al.* with the mean polarizability reported by Bulanin *et al.* gives a polarizability anisotropy of $\Delta\alpha \approx -0.19$, which is in excellent agreement with the calculations presented in the next section, and lower than the present value of $\Delta\alpha = -0.35$.

Since the mean polarizability is similar for all three molecules, the main contribution to the variation in the depolarization ratios is the polarizability anisotropy. Fluoroethane has the largest anisotropy as a result of the distortion of the electronic charge distribution due to the presence of the single fluorine atom. Hexafluoroethane has the smallest anisotropy, half that of ethane, due to the larger fluorine atoms with longer C–F bond lengths producing a less ellipsoidal molecule. From the calculations in the following section, the $\alpha_\perp$ component is slightly larger than the $\alpha_\parallel$ component, giving a negative $\Delta\alpha$ value, and suggesting that the long axis of the ellipsoid is perpendicular to the C–C bond. The $\alpha_\parallel$ and $\alpha_\perp$ components for hexafluoroethane were calculated

assuming a negative polarizability anisotropy, giving $\alpha_{\parallel} = 5.14 \pm 0.05$ and $\alpha_{\perp} = 5.49 \pm 0.05$. The polarizability components for ethane were also determined, giving $\alpha_{\parallel} = 5.52 \pm 0.02$ and $\alpha_{\perp} = 4.74 \pm 0.02$.

Table 6.3 includes literature values for ethane and is similar to a table given by Coonan [16], except that all the values have been recalculated using a mean polarizability of $\alpha = 5.00 \pm 0.05$. Some of these are direct measurements of ρ_0, but failure to exclude the vibrational Raman contribution from the depolarization ratio results in higher polarizability anisotropies. Other values are from the R_{20} method [17], Cotton-Mouton effect and microwave Zeeman effect studies [18,19], and a recent result derived from a combination of Cotton-Mouton effect and field-gradient birefringence experiments [16,20]. These experiments determine the polarizability anisotropy, from which a depolarization ratio can be derived using equations 1.7 and 1.10. The depolarization ratios calculated using this method have the vibrational Raman lines excluded.

From the table, it is clear that there is considerable variation within the $\Delta\alpha$ and ρ_0 values for ethane. When the vibrational Raman lines are included, the depolarization ratio obtained in the present work is in excellent agreement with the ratios reported by Bridge and Buckingham [4], and Ritchie and Stankey [21]. When the vibrational Raman lines are excluded, the ratio reported by Ritchie and Stankey is in reasonable agreement with the present ratio. Of concern is the recent determination of $\Delta\alpha$ by Coonan [16] from a combination of Cotton-Mouton effect and field-gradient birefringence studies. Coonan predicted a depolarization ratio of $100\rho_0 = 0.129 \pm 0.021$, which is comparable to the value for 489 nm determined by Monan *et al.* [17] using the R_{20} method. Correcting the ratio reported by Monan *et al.* for dispersion using the data of Bogaard *et al.* [5] gives a depolarization ratio for 632.8 nm of approximately $100\rho_0 = 0.09 \pm 0.02$ (the uncertainty has been doubled). A dispersion correction for the depolarization ratio reported by Haverkort *et al.* gives $100\rho_0 = 0.11 \pm 0.01$ (the uncertainty has been doubled). Therefore, once account is taken of dispersion, the agreement with the value reported by Coonan is worse, but still in much better agreement than with the present depolarization ratio. The Cotton-Mouton and microwave Zeeman effect study reported

Table 6.3 A comparison of depolarization ratios and polarizability anisotropies for ethane.[a]

Year	Method	λ	$100\rho_0$	$\Delta\alpha$	Reference
1966	Rayleigh scattering, vib. Raman lines included	632.8	0.198 ± 0.001	0.862 ± 0.009	[4]
1977	Rayleigh scattering, vib. Raman lines included	488.0	0.20 ± 0.01	0.867 ± 0.023	[26]
1978	Rayleigh scattering, vib. Raman lines included. ρ_0 corrected for 3% ethylene impurity	632.8	0.134 ± 0.003	0.709 ± 0.011	[5]
1979	Rayleigh scattering, vib. Raman lines included	632.8	0.149 ± 0.006	0.748 ± 0.017	[27]
1982	Rayleigh scattering and R_{20} method, vib. Raman lines excluded	488.0	0.114 ± 0.010	0.654 ± 0.029	[17]
1983	Rayleigh scattering, vib. Raman lines excluded	514.5	0.135 ± 0.003	0.71 ± 0.01	[13]
1983/4	Cotton-Mouton effect and microwave Zeeman effect, vib. Raman lines excluded	632.8	0.176 ± 0.037	0.816 ± 0.086	[18,19]
1991	Rayleigh scattering, vib. Raman lines included	632.8	0.191 ± 0.008	0.847 ± 0.020	[21]
1991	Rayleigh scattering, vib. Raman lines excluded	632.8	0.150 ± 0.014	0.751 ± 0.036	[21]
1995	Cotton-Mouton effect and field-gradient birefringence, vib. Raman lines excluded	632.8	0.129 ± 0.021	0.698 ± 0.056	[16]
1995	Rayleigh scattering, vib. Raman lines included	632.8	0.199 ± 0.002	0.865 ± 0.010	Present study
1995	Rayleigh scattering, vib. Raman lines excluded	632.8	0.159 ± 0.002	0.773 ± 0.010	Present study

[a] The values were recalculated using a mean polarizability of $\alpha = 5.00 \pm 0.05$.

by Hüttner and co-workers gives a depolarization ratio of $100\rho_0 = 0.176 \pm 0.037$, which is higher than the value reported by Coonan, and is comparable to the present light scattering result.

Overall, there is poor agreement amongst the values, but it is evident that the depolarization ratio of ethane is within the range $100\rho_0 = 0.13$ to 0.16. Unfortunately, the two most recent determinations are at opposite extremes of the range, and it is debatable which value is correct. A direct measurement of the depolarization ratio, with exclusion of the vibrational Raman lines, should be reasonably accurate if the instrumental depolarization is either negligible (as assumed here) or taken into account. In comparison, studies of the temperature dependence of the Cotton-Mouton effect are required to separate the temperature dependent and independent contributions to that effect. A plot of ${}_{m}C$ against T^{-1} gives a slope proportional to $\Delta\alpha\Delta\chi$ (equation 1.35), and weighted-fit least-squares analysis is used to determine the gradient, but a large temperature range is necessary for precise results.

A study of the other haloethanes has been completed by Ritchie *et al.* [1], where light scattering, Kerr effect and computational data were combined to obtain the experimental polarizability components. Table 6.4 reports the depolarization ratios and mean polarizabilities for the haloethanes. The mean polarizabilities from Ritchie *et al.* were recalculated from the original data using density second virial coefficients from the literature [2] and are comparable to values derived from refractive indices [22]. The method of Pitzer [23] was used to estimate the density second virial coefficients for iodoethane, giving $B(340\ \text{K}) = -749 \times 10^{-6}\ \text{m}^3\ \text{mol}^{-1}$, $B(360\ \text{K}) = -684 \times 10^{-6}\ \text{m}^3\ \text{mol}^{-1}$. As expected the mean polarizability increases as a function of the size of the halogen. Since the depolarization ratio also increases along the series, the anisotropy in the electronic charge distribution is increasing at a greater rate than the mean polarizability.

Table 6.4 Depolarization ratios and mean polarizabilities for the haloethanes.[a]

	$100\rho_0$	α
fluoroethane	0.227 ± 0.002	5.00 ± 0.05
chloroethane	0.579 ± 0.002	7.14 ± 0.07
bromoethane	0.806 ± 0.005	8.34 ± 0.08
iodoethane	0.976 ± 0.004	10.7 ± 0.1

[a] The depolarization ratios have the vibrational Raman lines excluded. Except for fluoroethane, the results are from Ritchie *et al.* [1].

Theoretical calculations

Ab initio calculations were undertaken for hexafluoroethane to resolve the discrepancy between the present mean polarizability and the value reported by Bulanin *et al.* Furthermore, the calculations were expected to provide some insight into the contribution from the polarizability components, as was shown in the discussion above.

The geometry for hexafluoroethane was optimized using the GAMESS program with the 6-31G* basis set, giving C–C = 0.1530 (0.1545) nm, C–F = 0.1340 (0.1326) nm and C–C–F = 109.7° (109.75°). The values in parentheses are from an electron diffraction study [24]. The C–C bond length is shorter for the calculated geometry, but the C–F bond length is longer. The bond angles are in good agreement and, overall, the optimized geometry gives a slightly larger molecule than the r_g geometry, which is an average over thermal vibrations.

The polarizabilities were calculated using the CHF method with the 6-31G(+sd+sp) basis set, and MP2 corrections were calculated by the finite-field method. Zero-frequency and optical-frequency polarizabilities are given in Table 6.5, and zero-frequency polarizabilities for ethane calculated by Spackman [15] using the 6-31G(+sd+sp) basis set are also included. A summary of frequency-dependent polarizabilities at the SCF and MP2 levels of theory for selected laser frequencies is given in Appendix I.

For hexafluoroethane, the $\alpha_\perp$ component is slightly larger than the $\alpha_\parallel$ component, whereas in ethane the $\alpha_\parallel$ component is much larger than the $\alpha_\perp$ component. This is a result of the longer C–F bond and smaller C–C–F angle, which allows greater polarization in the direction of the $\alpha_\perp$ component. The optical-frequency MP2 mean polarizability is 11% lower than the polarizability obtained in the present study, and 5% lower than the value reported by Bulanin *et al.* From this result, it is probable that the mean polarizability obtained in the present research is too large, which explains why the mean polarizability reported by Bulanin *et al.* was used in the derivation of $\Delta\alpha$. The optical-frequency MP2 values of α and α_{--} are smaller than the experimental values by 4 and 7%, respectively, and the $\Delta\alpha$ value is approximately half of the experimental value.

Table 6.5 Calculated polarizability components for ethane and hexafluoroethane using the 6-31G(+sd+sp) basis set.

		λ(nm)	$\alpha_\perp$	$\alpha_\parallel$	α	$\Delta\alpha$
C_2H_6[a]	SCF	∞	4.258	4.810	4.442	0.551
	MP2	∞	4.419	5.061	4.633	0.642
C_2F_6	SCF	∞	4.570	4.372	4.504	–0.198
		632.8	4.604	4.405	4.538	–0.199
	MP2	∞	5.115	4.928	5.053	–0.187
		632.8	5.149	4.961	5.086	–0.188

[a] Reference [15].

The quadrupole moment for hexafluoroethane was calculated as an energy derivative at the MP2 level of theory giving Θ = 1.47 x 10^{-40} C m^2. This is smaller and opposite in sign to the quadrupole moment for ethane of Θ = (–2.25 ± 0.15) x 10^{-40} C m^2 reported by Watson [20] from a study of the temperature dependence of the field-gradient birefringence. The quadrupole moment for ethane of Θ = –3.05 x 10^{-40} C m^2 calculated by Spackman [15] at the MP2 level of theory using the 6-31G(+sd+sp) basis set is larger than the experimental value. Therefore, it is expected that the quadrupole

moment for hexafluoroethane noted above is also too large. A change in sign for the quadrupole moment for hexafluoroethane with respect to ethane is expected since the electronegative fluorine atoms shift the electronic charge distribution away from the carbon-carbon bond, and there is also a variation in the bond angles.

Conclusions

The depolarization ratio, mean polarizability and polarizability anisotropy were reported for ethane. Despite excellent agreement with other light scattering results, the depolarization ratio and polarizability anisotropy disagree with a recent value deduced by Coonan [16] from a combination of Cotton-Mouton and field-gradient birefringence experiments.

The depolarization ratio and polarizability anisotropy for fluoroethane were determined for the first time. The results for fluoroethane complete the light scattering measurements on the haloethanes, and complement a study of the gas-phase Kerr effect of this molecule by Blanch and Ritchie [25]. The depolarization ratio for hexafluoroethane differs markedly from the value reported by Haverkort *et al.* [13]. The depolarization ratio for hexafluoroethane is extremely small, so it is possible that instrumental depolarization may be contributing to the final result. Chapter 10 includes a discussion of the evaluation of the instrumental depolarization for the present apparatus. The mean polarizability for hexafluoroethane disagrees with the values reported by Bulanin *et al.* [12] and Haverkort *et al.* [13]. More experimental research and higher-level calculations are necessary to solve the discrepancies amongst the hexafluoroethane values.

References

1. Ritchie, G.L.D., Spackman, M.A. and Stankey, R., unpublished results.
2. Dymond, J.H. and Smith, E.B., *"The virial coefficients of pure gases and mixtures"*, (Oxford University Press, Oxford, 1980).
3. Bignell, C.M. and Dunlop, P.J , *J. Chem. Phys.*, **98**, 4889 (1993).
4. Bridge, N.J. and Buckingham, A.D., *Proc. Roy. Soc. A*, **295**, 334 (1966).
5. Bogaard, M.P., Buckingham, A.D., Pierens, R.K. and White, A.H., *J. Chem. Soc., Faraday Trans. 1*, **74**, 3008 (1978).
6. Jhanwar, B.L., Meath, W.J. and MacDonald, J.C.F., *Can. J. Phys.*, **59**, 185 (1981).
7. Kerl, K. and Haüssler, H., *Ber. Bunsen Ges. Phys. Chem.*, **88**, 992 (1984).
8. Achtermann, H.J. and Magnus, G., *J. Chem. Phys.*, **94**, 5669 (1991).
9. Hohm, U., *Mol. Phys.*, **78**, 925 (1993).
10. Weast, R.C., *"CRC Handbook of Chemistry and Physics"*, 70th Edition (CRC Press, Boca Raton, 1990).
11. Maryott, A.A. and Buckley, F., *"Table of dielectric constants and electric dipole moments of substances in the gaseous state."*, (National Bureau of Standards, Washington, 1953).
12. Bulanin, M.O., Burtsev, A.P. and Tretyakov, P.Y., *Opt. Spectrosc. (USSR)*, **69**, 760 (1990).
13. Haverkort, J.E.M., Baas, F and Beenakker, J.J.M., *Chem. Phys.*, **79**, 105 (1983).
14. Bishop, D.M. and Cheung, L.M., *J. Phys. Chem.*, **11**, 119 (1982).
15. Spackman, M.A., *J. Phys. Chem.*, **93**, 7594 (1989).
16. Coonan, M.H., *"Temperature dependence of the Cotton-Mouton effect in gases"*, Ph.D. Thesis, University of New England, (1995).
17. Monan, M., Bribes, J.L. and Gaufrès, R., *J. Raman Spectrosc.*, **12**, 190 (1982).
18. Kling, H., Geschka, H. and Hüttner, W., *Chem. Phys. Lett.*, **96**, 631 (1983).
19. Hüttner, W., Häussler, H. and Majer, W., *Chem. Phys. Lett.*, **109**, 359 (1984).

20. Watson, J.N., *"The measurement of field-gradient induced birefringence in gases"*, Ph.D. Thesis, University of New England, (1994).

21. Ritchie, G.L.D. and Stankey, R., unpublished results.

22. Landolt-Börnstein, *"Numerical data and functional relationships in science and technology"*, Volume II/8 (Springer-Verlag, Berlin, 1962).

23. Pitzer, K.S., *J. Am. Chem. Soc.*, **77**, 3427 (1955).

24. Gallaher, K.L., Yokozeki, A. and Bauer, S.H., *J. Phys. Chem.*, **78**, 2389 (1974).

25. Blanch, E.W. and Ritchie, G.L.D., unpublished results.

26. Burnham, A.K., Buxton, L.W. and Flygare, W.H., *J. Chem. Phys.*, **67**, 4990 (1977).

27. Baas, F. and van den Hout, K.D., *Physica*, **95**, 597 (1979).

Chapter Seven

Acetylene, methylacetylene, dimethylacetylene and hexafluoro-2-butyne

Introduction

Acetylene is the simplest molecule containing a carbon-carbon triple bond, and the study of the electric and magnetic properties of this molecule has a long history [1]. Kerr effect [2], Cotton-Mouton effect [1,3], microwave Zeeman effect [4,5], and field-gradient birefringence results [6] have been reported for acetylene. Studies of the temperature dependence of the Kerr and Cotton-Mouton effects of methylacetylene and dimethylacetylene are as yet unreported [7,8]. Methylacetylene has been studied by the microwave Zeeman effect [9,10], and a single-temperature Kerr effect study has been reported [11].

Depolarization ratios for acetylene, methylacetylene and dimethylacetylene have been reported by several research groups [12-15]. The literature values for acetylene are in satisfactory agreement and, although difficult to handle, this compound was chosen, in the present work, as a secondary standard to check the linearity of the photomultiplier tube and photon counting system to changes in scattering intensities. There is considerable disagreement amongst the values reported for methylacetylene and dimethylacetylene by Bogaard *et al.* [15] and Alms *et al.* [12]. A study of these molecules was therefore initiated to resolve the discrepancy. The polarizability anisotropies for acetylene, methylacetylene and dimethylacetylene determined in the

present work are combined with results of studies of the Cotton-Mouton effect and field-gradient birefringence effect to obtain the quadrupole moments, quadrupole hyperpolarizabilities, magnetizability anisotropies, and magnetic hyperpolarizability anisotropies of these molecules. A study of hexafluoro-2-butyne was included to complement the investigation of fluorine substitution for ethane, fluoroethane and hexafluoroethane presented in Chapter 6. Computational interest in this series of molecules has focused on acetylene. Due to its relatively small size, the use of large basis sets and high levels of theory have been possible [16-21], and vibrational averages of the electric properties have been reported [22,23]. Ab initio calculations for acetylene, methylacetylene and dimethylacetylene have been included in the present work.

Experimental details

Acetylene (> 99.6%) and methylacetylene were obtained from Matheson Gas Products; dimethylacetylene (> 99%) was obtained from the Aldrich Chemical Company; and hexafluoro-2-butyne was obtained from the Pierce Chemical Company. Acetone was removed from acetylene by passing the gas through two vapour traps immersed in an ice-salt bath. The purities of methylacetylene, dimethylacetylene and hexafluoro-2-butyne were determined to be > 99.99%, > 99.6% and > 99.85%, respectively, from gas-chromatographic analyses. All four gases were used without further purification.

A summary of the depolarization ratios obtained for acetylene, methylacetylene, dimethylacetylene and hexafluoro-2-butyne, with inclusion and exclusion of the vibrational Raman lines, is given in Table 7.1. The ratios were recorded at room temperature with Version 2 of the apparatus. Integration times for acetylene and hexafluoro-2-butyne were 100 s for the polarized component and 200 s for the depolarized component. Integration times were doubled for dimethylacetylene, and varying times of up to 500 s for the polarized component and 1 000 s for the depolarized component were used for methylacetylene.

For acetylene, methylacetylene and dimethylacetylene, the ratios given in Table 7.1 are a combination of two sets of results with periods of three to twelve months

between the recording of the data. For acetylene at ≈ 100 kPa, typical polarized and depolarized counts, with inclusion of the vibrational Raman lines, were 29 880 and 548 cps, with background counts of 17 and 3 cps respectively. Typical polarized and depolarized counts for methylacetylene at ≈ 100 kPa, with inclusion of the vibrational Raman lines, were 94 130 and 2 060 cps, with background counts of 26 and 8 cps, respectively. At room temperature the vapour pressure of dimethylacetylene was limited to ≈ 50 kPa. Typical polarized and depolarized counts, with inclusion of the vibrational Raman lines, were 96 620 and 2 594 cps, with background counts of 24 and 3 cps, respectively. For hexafluoro-2-butyne, typical polarized and depolarized counts at ≈ 100 kPa, with inclusion of the vibrational Raman lines, were 148 300 and 2 400 cps, with background counts of 22 and 4 cps respectively.

Density second virial coefficients for acetylene and methylacetylene were taken from the literature [24]. The method of Pitzer [25] was used to calculate the virial coefficients of dimethylacetylene, giving $B(290\ \mathrm{K}) = -838.5 \times 10^{-6}\ \mathrm{m^3\ mol^{-1}}$ and $B(300\ \mathrm{K}) = -776.5 \times 10^{-6}\ \mathrm{m^3\ mol^{-1}}$. Virial coefficients were unavailable for hexafluoro-2-butyne.

Discussion

The ratios presented in Table 7.1 are of high precision giving mean depolarization ratios with small uncertainties. The depolarization ratios, mean polarizabilities and polarizability anisotropies are given in Table 7.2, and literature values are included. The vibrational Raman contributions to the depolarization ratios were found to be ≈ 4% for acetylene, ≈ 6% for methylacetylene and ≈ 1.5% for dimethylacetylene. The vibrational Raman contribution was found to be negligible for hexafluoro-2-butyne.

The depolarization ratio for acetylene, with inclusion of the vibrational Raman lines, is in excellent agreement with the value for 647.1 nm reported by Alms *et al.* [12], and also with the value for 632.8 nm reported by Baas and van den Hout [13], although the uncertainty in this value is large. The ratio differs from the value reported by Bridge and Buckingham [14], which is surprising since only Bridge and Buckingham mentioned

trapping of acetone from the acetylene gas sample. Without the trapping of acetone, the depolarization ratio for acetylene, with inclusion of the vibrational Raman lines, gave $100\rho_0 = 1.85 \pm 0.02$ (mean of seven values not reported here) compared to the value of $100\rho_0 = 1.81 \pm 0.02$ for the purified gas.

Table 7.1 Depolarization ratios for acetylene, methylacetylene, dimethylacetylene and hexafluoro-2-butyne.

$100\rho_0$			
C_2H_2	C_3H_4	C_4H_6	C_4F_6
1.812 ± 0.009	2.187 ± 0.003	2.673 ± 0.004	1.589 ± 0.003
1.801 ± 0.006	2.180 ± 0.003	2.661 ± 0.005	1.589 ± 0.003
1.795 ± 0.007	2.254 ± 0.004	2.668 ± 0.004	1.615 ± 0.003
1.806 ± 0.008	2.204 ± 0.004	2.667 ± 0.004	1.611 ± 0.003
1.804 ± 0.009	2.223 ± 0.004	2.679 ± 0.004	1.595 ± 0.003
1.796 ± 0.009	2.228 ± 0.005	2.668 ± 0.004	1.607 ± 0.003
1.803 ± 0.009	2.221 ± 0.005	2.667 ± 0.004	1.616 ± 0.004[a]
1.815 ± 0.009	2.236 ± 0.005	2.667 ± 0.004	1.625 ± 0.004[a]
1.833 ± 0.009	2.214 ± 0.005	2.671 ± 0.005	1.574 ± 0.004[a]
1.824 ± 0.009	2.116 ± 0.005[a]	2.681 ± 0.005	1.613 ± 0.004[a]
1.737 ± 0.009[a]	2.099 ± 0.005[a]	2.619 ± 0.005[a]	1.621 ± 0.004[a]
1.738 ± 0.009[a]	2.088 ± 0.005[a]	2.639 ± 0.005[a]	1.619 ± 0.004[a]
1.745 ± 0.008[a]	2.086 ± 0.003[a]	2.623 ± 0.005[a]	
1.731 ± 0.009[a]	2.076 ± 0.003[a]	2.633 ± 0.005[a]	

[a] Vibrational Raman lines excluded.

The depolarization ratio for methylacetylene, with inclusion of the vibrational Raman lines, agrees with the value for 632.8 nm reported by Bogaard *et al.* [15], but does not agree with the ratio for 647.1 nm reported by Alms *et al.* [12]. The depolarization ratio for dimethylacetylene, with inclusion of the vibrational Raman lines,

is smaller than the value for 647.1 nm reported by Alms *et al.*, and also smaller than the value for 514 nm reported by Bogaard *et al.* The depolarization ratios reported by Bogaard *et al.* were extrapolated to 632.8 nm giving $100\rho_0 = 2.70$, which is in good agreement with the present ratio, although the extrapolation introduces a large uncertainty. For dimethylacetylene, it is probable that the values reported by Bogaard *et al.* are more reliable than those reported by Alms *et al.*

Except for hexafluoro-2-butyne, only one mean polarizability was determined for each molecule with exclusion of the vibrational Raman lines. In the case of acetylene, the present mean polarizability is in poor agreement with the literature values, which are expected to be very reliable. The mean polarizability of methylacetylene is higher than values derived from refractive indices [15] and measurements of the relative permittivity [26]. For dimethylacetylene, agreement with literature values is again poor, although this is aggravated by determinations at different wavelengths. Since it is suspected that the mean polarizabilities measured in the present work are too large, the literature values of $\alpha = 3.88 \pm 0.08$ for acetylene, $\alpha = 6.35 \pm 0.13$ for methylacetylene and $\alpha = 8.19 \pm 0.16$ for dimethylacetylene were used in the derivation of $\Delta\alpha$, $\alpha_{\parallel}$ and $\alpha_{\perp}$, where an uncertainty of $\pm$ 2% has been assumed for all three molecules. Finally, the differing depolarization ratios and mean polarizabilities are reflected in the polarizability anisotropies, where the agreement is poor. For methylacetylene and dimethylacetylene, $\Delta\alpha$ lies between the literature values of Bogaard *et al.* and Alms *et al.*

As with carbon dioxide and fluoroethane, the precision of the mean polarizability was investigated for hexafluoro-2-butyne. In this case, two different laser line filters were used, as well as no filter, and the results are given in Table 7.2. The mean polarizabilities which excluded the vibrational Raman lines are 1.5% higher than the mean polarizabilities which included the lines, but a greater number of data points would be required to permit valid statistical analysis. The difference between the two sets of results which exclude the lines is negligible, which rules out a defective filter. In the derivation of $\Delta\alpha$, $\alpha_{\parallel}$ and $\alpha_{\perp}$, the average of the five mean polarizabilities ($\alpha = 9.42 \pm 0.28$) which excluded the vibrational Raman lines was used, where an uncertainty of $\pm$ 3% was

Table 7.2 Depolarization ratios, mean polarizabilities and polarizability anisotropies of acetylene, methylacetylene, dimethylacetylene, and hexafluoro-2-butyne.

Molecule	λ(nm)	$100\rho_0$	α	$\Delta\alpha$	Reference
HCCH	632.8	1.81 ± 0.02			Present study
	632.8	1.737 ± 0.006[a]	3.98 ± 0.04[a]	2.00 ± 0.04[b]	Present study
	632.8	1.79 ± 0.05			[13]
	647.1	1.81 ± 0.03	3.86	2.04	[12]
	632.8	1.851 ± 0.004			[14]
	632.8		3.88	2.072	[15]
	632.8		3.88		[27]
	∞		3.87[c]		[26]
CH_3CCH	632.8	2.22 ± 0.03			Present study
	632.8	2.09 ± 0.02[a]	6.41 ± 0.07[a]	3.61 ± 0.08[b]	Present study
	647.1	2.04 ± 0.02	6.35	3.56	[12]
	632.8	2.25 ± 0.02	6.35	3.75	[15]
	∞		6.29[c]		[26]
CH_3CCCH_3	632.8	2.670 ± 0.006			Present study
	632.8	2.63 ± 0.01[a]	8.81 ± 0.09[a]	5.24 ± 0.10[b]	Present study
	647.1	2.73 ± 0.03	7.69	5.01	[12]
	514.5	2.79 ± 0.0	8.19	5.47	[15]
	589		8.22[d]		[28]
CF_3CCCF_3	632.8	1.60 ± 0.02	9.31 ± 0.04		Present study
	632.8	1.61 ± 0.006[a]	9.29 ± 0.05	4.66 ± 0.14	Present study
	632.8		9.40 ± 0.04[a]		Present study
	632.8		9.37 ± 0.06[a]		Present study
	632.8		9.48 ± 0.05[a]		Present study
	632.8		9.44 ± 0.06[e]		Present study
	632.8		9.41 ± 0.06[e]		Present study

[a] Vibrational Raman lines excluded.
[b] Derived using the present depolarization ratios, which excluded the vibrational Raman lines, and mean polarizabilities obtained from the literature (see text).
[c] These values include a vibrational polarizability correction [29].
[d] Liquid-phase refractive index value.
[e] Vibrational Raman lines excluded but a different laser line filter used.

assumed. This value was used with caution, because the mean polarizabilities obtained for the other acetylenes in this work were too high. No explanation can be offered for the observation of higher mean polarizabilities when the vibrational Raman lines are excluded except to mention that, to a good approximation, exclusion of the vibrational Raman lines should not affect the determination of the mean polarizability using the present method.

The polarizability components for the four species are summarized in Table 7.3. Progressive insertion of methyl groups results in simple additivity for the polarizability anisotropies of acetylene, methylacetylene and dimethylacetylene. Although the methyl group contributes more to the $\alpha_{\parallel}$ component for dimethylacetylene than methylacetylene, and the reverse applies for the $\alpha_{\perp}$ component, these balance to give an increment of ≈ 1.6 in the polarizability anisotropies. Fluorine substitution into dimethylacetylene to give hexafluoro-2-butyne gives results similar to those obtained for ethane and hexafluoroethane. Due to the longer C–F bond, the $\alpha_{\perp}$ component is larger than the $\alpha_{\parallel}$ component for hexafluoro-2-butyne relative to dimethylacetylene. This results in a smaller polarizability anisotropy and a smaller depolarization ratio.

Table 7.3 Polarizability components for acetylene, methylacetylene, dimethylacetylene, and hexafluoro-2-butyne.

Molecule	$\alpha_{\parallel}$	$\alpha_{\perp}$
HCCH	5.22 ± 0.09	3.21 ± 0.08
CH_3CCH	8.75 ± 0.15	5.15 ± 0.13
CH_3CCCH_3	11.68 ± 0.20	6.44 ± 0.16
CF_3CCCF_3	12.5 ± 0.3	7.9 ± 0.3

Studies of the temperature dependence of the Cotton-mouton effect of acetylene, methylacetylene and dimethylacetylene have been reported [1,3,8]. From equation 1.35, it is clear that a plot of ${}_{m}C$ against T^{-1} will give the magnetic hyperpolarizability anisotropy, $\Delta\eta$, from the intercept, and a gradient proportional to the product $\Delta\alpha\Delta\chi$.

Therefore, if the polarizability anisotropy is known from Rayleigh light scattering, then the magnetizability anisotropy can be derived.

If the moment of inertia and rotational g value are known then the quadrupole moment for a rigid, linear molecule can be calculated by rearranging equation 1.36 to give

$$\Theta = \frac{eIg}{m_p} - \left(\frac{4m_e}{e}\right)\Delta\chi \tag{7.1}$$

The quadrupole moment for a rigid, axially symmetric molecule can be calculated using

$$\Theta = -\frac{e}{m_p}(g_{\parallel}I_{\parallel} - g_{\perp}I_{\perp}) - \left(\frac{4m_e}{e}\right)\Delta\chi \tag{7.2}$$

where $g_{\parallel}$ and $g_{\perp}$ are the rotational g values and $I_{\parallel}$ and $I_{\perp}$ are the principal moments of inertia parallel and perpendicular to the axis of symmetry.

The results of the studies of the temperature dependence of the Cotton-Mouton effects of acetylene, methylacetylene and dimethylacetylene are given in Figure 7.1, where the data for acetylene are from Coonan and Ritchie [1] and the data for methylacetylene and dimethylacetylene are from Lamb and Ritchie [8]. The experimental procedures and design are as described in the literature [30,31] and will not be discussed here. The results of the measurements are summarized in Table 7.4, where the uncertainties shown are based on the standard deviations derived from weighted-fit least-squares analyses.

For acetylene, the magnetizability anisotropy derived in the present analysis is 3.5% higher in absolute terms than the value reported by Coonan and Ritchie, due to the lower polarizability anisotropy obtained in the present work, but this is within the quoted uncertainties. The magnetizability anisotropy was combined with the moment of inertia and rotational g value to give a quadrupole moment of Θ = (20.4 ± 1.4) x 10^{-40} C m^2, which is 1.5% higher than the value reported by Coonan and Ritchie. This results in slightly poorer agreement with the quadrupole moments of Θ = (19.7 ± 1.0) x 10^{-40} C m^2 and Θ = (18.1 ± 1.4) x 10^{-40} C m^2 reported by Watson [6] from a study of the

field-gradient birefringence effect and Dagg *et al.* [32] from studies of the collision-induced infrared absorption. Other values derived from the magnetizability anisotropy using the microwave Zeeman effect [4,5] and the Cotton-Mouton effect [3] are too high.

Watson [6] derived the quadrupole moment using a polarizability anisotropy of $\Delta\alpha = 2.072 \pm 0.062$ from light scattering data reported by Bogaard *et al.* [15], but this value of the polarizability anisotropy has been shown in the present work to be too high. Recalculation of the quadrupole moment using the polarizability anisotropy given in Table 7.4 gives $\Theta = (20.4 \pm 1.3) \times 10^{-40}$ C m^2, which is in excellent agreement with the value derived from the Cotton-Mouton effect. The quadrupole moment can also be corrected by using an estimate of the quadrupole hyperpolarizability from calculations by Maroulis and Thakkar [16]. They found that B contributed –7% to the value of ${}_{m}Q$ at 294 K. Therefore, a corrected value of the quadrupole moment is $\Theta = (21.9 \pm 1.3) \times 10^{-40}$ C m^2.

Russell and Spackman [22] report a similar calculation in a theoretical study of acetylene. The theoretical calculations reported by Russell and Spackman are vibrationally and thermally averaged, and used large, carefully selected basis sets and high levels of theory. Certainly, the quadrupole moment of $\Theta = 21.16 \times 10^{-40}$ C m^2 obtained is very precise and current experimental methods cannot reach this level of accuracy. Other ab initio calculations using different levels of electron correlation and vibrational averaging [17,23,33,34] lend support to the above value.

For methylacetylene, the magnetizability anisotropy was determined to be $\Delta\chi = (-13.52 \pm 0.81) \times 10^{-29}$ J T^{-2}. Combining $\Delta\chi$ with the moments of inertia and the rotational g values gives a quadrupole moment of $\Theta = (18.3 \pm 1.9) \times 10^{-40}$ C m^2. This value is 13.6% higher than the quadrupole moment of $\Theta = (16.1 \pm 0.8) \times 10^{-40}$ C m^2 reported by Shoemaker and Flygare [10] from a study of the microwave Zeeman effect. The present value is in much better agreement with the quadrupole moment of $\Theta_{QC} = (18.4 \pm 0.9) \times 10^{-40}$ C m^2 reported by Watson. Unfortunately, for dipolar molecules the values are not directly comparable, since quadrupole moments obtained from the Cotton-Mouton and microwave Zeeman effects through equation 7.2 are derived

with respect to the centre of mass whereas the quadrupole moment obtained from the field-gradient birefringence is der ved with respect to the effective quadrupole centre. Nonetheless, it is evident that the quadrupole moment reported by Shoemaker and Flygare is too low.

Rotational g values for dimethylacetylene are unknown, therefore, a quadrupole moment cannot be determined from the Cotton-Mouton effect measurements. Since this is the first reported study of the temperature dependence of the molar field-gradient birefringence constant for dimethylacetylene, comparisons cannot be made with the present value of the quadrupole mo nent.

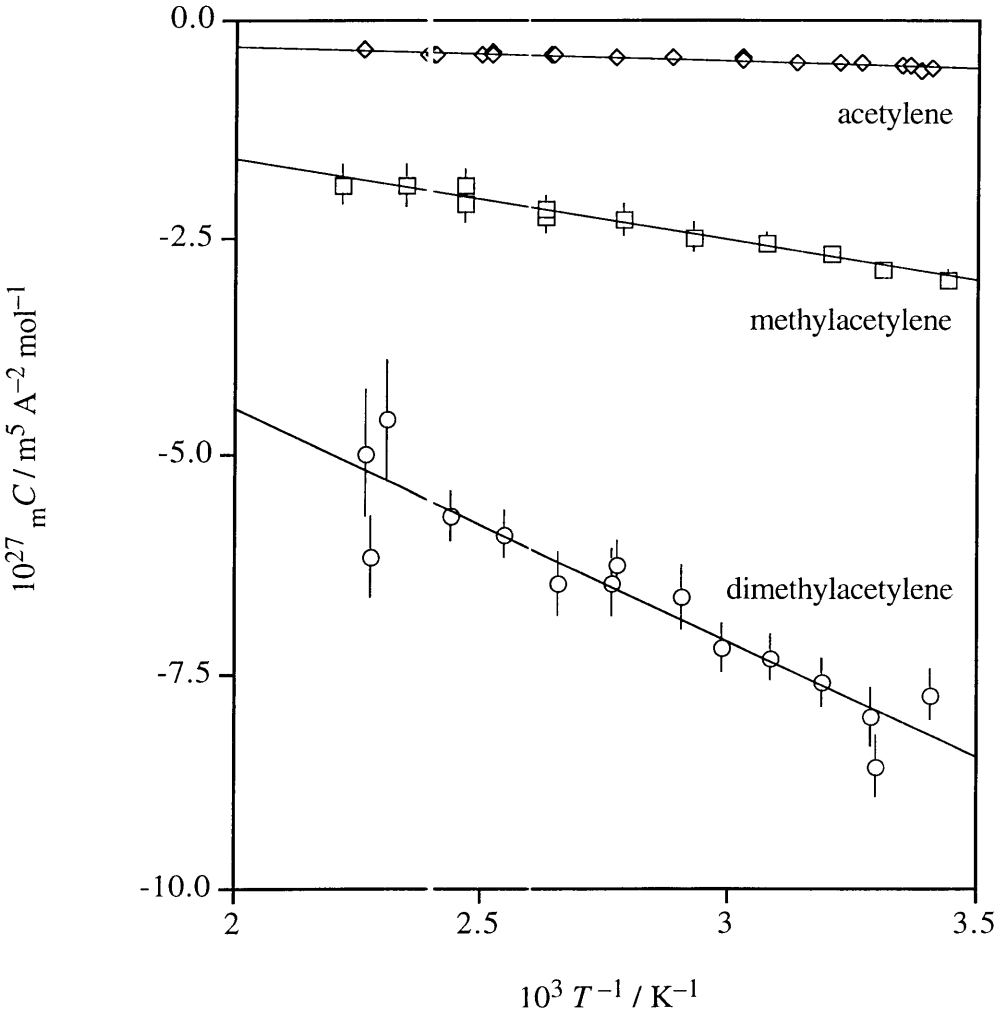

Figure 7.1 Temperature dependence of the Cotton-Mouton effects of acetylene, methylacetylene and dimethylacetylene.

Table 7.4 Analysis of the temperature dependence of the Cotton-Mouton effects of acetylene, methylacetylene and dimethylacetylene.

	acetylene	methylacetylene	dimethylacetylene	Reference
$100\rho_0$	1.737 ± 0.006	2.09 ± 0.02	2.63 ± 0.01	Present work
α	3.88 ± 0.08	6.35 ± 0.13	8.19 ± 0.16	[15]
$\Delta\alpha$	2.00 ± 0.04	3.61 ± 0.08	5.24 ± 0.10	
10^{24} slope / $m^5\ A^{-2}\ mol^{-1}\ K$	−0.157 ± 0.010	−0.938 ± 0.052	−2.646 ± 0.286	[1,8]
10^{27} intercept / $m^5\ A^{-2}\ mol^{-1}$	0.011 ± 0.030	0.277 ± 0.146	0.814 ± 0.815	[1,8]
$10^{50}\ \Delta\eta$ / $C\ m^2\ V^{-1}\ T^{-2}$	3 ± 8	70 ± 37	204 ± 205	[1,8]
$10^{29}\ \Delta\chi$ / $J\ T^{-2}$	−4.08 ± 0.27	−13.52 ± 0.81	−26.29 ± 2.9	[1,8]
B_0 / MHz	35273.8	159142.1 ($B_\parallel$)	3363.16	[35,37,38]
		8545.87712 ($B_\perp$)		
g	0.04903 ± 0.00004	0.312 ± 0.002 ($g_\parallel$)		[10,39]
		0.00350 ± 0.00015 ($g_\perp$)		
$10^{46}\ I$ / $kg\ m^2$	2.379109	0.5273288 ($I_\parallel$)		
		9.819966 ($I_\perp$)		
$10^{40}\ \Theta$ / $C\ m^2$	20.4 ± 1.4	18.3 ± 1.9		

The magnetic hyperpolarizability anisotropies determined in the present analysis are poorly defined. The contributions to the Cotton-Mouton constants at 298 K from the temperature independent terms are $\approx -2\%$ for acetylene and $\approx -10\%$ for methylacetylene and dimethylacetylene, which indicates that a study of the temperature dependence was justified. As mentioned by Coonan and Ritchie [31], it is possible that the magnetic hyperpolarizability anisotropy may be proportional to the mean polarizability, since the magnetic hyperpolarizability tensor describes the quadratic response of the electric polarizability tensor to an applied magnetic induction. It is difficult to see any definite trend, although the values do increase as the mean polarizability increases.

Theoretical calculations

Calculations of the polarizability components for acetylene, methylacetylene, and dimethylacetylene were included to complement the experimental results. The geometries of methylacetylene and dimethylacetylene were optimized at the MP2 level of theory using the 6-31G** basis set, and are given in Table 7.5. The optimized methylacetylene structure is in excellent agreement with a near-equilibrium geometry [35]. The dimethylacetylene optimized structure has shorter methyl C–H and C–C bond lengths, while the triple bond is slightly longer when compared to the r_g structure (where the internuclear distances are averaged over the thermal vibrations) [36]. The MP2/6-31G** optimized geometry for acetylene was obtained from the literature [34].

Optical-frequency polarizability components for acetylene, methylacetylene, and dimethylacetylene at the SCF and MP2 levels of theory are given in Table 7.6. The polarizabilities were calculated using the CHF method with the CADPAC program. A summary of frequency dependent polarizabilities at common laser frequencies is given in Appendix I for all three molecules.

For methylacetylene and dimethylacetylene, problems were encountered with convergence of the SCF energies. To obtain convergence, it was necessary to alter the d exponent on the heavy atom from 0.175 to 0.25 giving the 6-31G(+sd+sp)$_e$ and 6-31G(+pd+sp)$_e$ basis sets. From Table 7.6, the effect of a less diffuse d function for

methylacetylene is polarizability components with greater similarity to the 6-31G(+sd+sp) basis set calculations, and not those of the unaltered 6-31G(+pd+sp) basis set. In effect, the tighter d function restricts the relaxation of the valence electrons. For all three basis sets, the MP2 corrected polarizability components for methylacetylene give larger $\alpha_{\perp}$ and smaller $\alpha_{\parallel}$ components than the SCF values. The mean polarizabilities do not differ significantly, whereas the polarizability anisotropies are smaller at the MP2 level of theory.

Table 7.5 Comparison of optimized and experimental geometries of methylacetylene and dimethylacetylene.[a]

		MP2/6-31G**	Experiment[b]
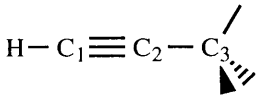	$H–C_1$	0.1061	0.1061
	$C_1–C_2$	0.1218	0.1204
	$C_2–C_3$	0.1460	0.1458
	$C_3–H$	0.1088	0.1088
	$C_2–C_3–H$	110.83°	110.83
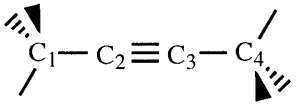	H–C	0.1088	0.1116
	$C_1–C_2$	0.1461	0.1467
	$C_2–C_3$	0.1220	0.1213
	$C_2–C_1–H$	111.01°	110.7

[a] Bond lengths are in nm.

[b] The r_g structure for dimethylacetylene is from reference [36] and the near-equilibrium structure for methylacetylene is from reference [35].

For acetylene, the effect of replacing the diffuse s function with a p function having the same exponent, giving the 6-31G(+pd+sp) basis set, results in little change to the $\alpha_{\parallel}$ component. The out-of-plane component increases significantly due to the presence of the p function, which allows relaxation of the electrons above the carbon-

Table 7.6 SCF and MP2 polarizability components for acetylene, methylacetylene and dimethylacetylene at 632.8 nm.[a]

	SCF				MP2			
	$\alpha_\perp$	$\alpha_\parallel$	α	$\Delta\alpha$	$\alpha_\perp$	$\alpha_\parallel$	α	$\Delta\alpha$
acetylene								
6-31G(+pd+sp)	3.037	5.451	3.842	2.414	3.016	5.221	3.751	2.205
					(3.21)	(5.22)	(3.88)	(2.00)
methylacetylene								
6-31G(+sd+sp)	4.490	8.412	5.797	3.922	4.546	8.288	5.793	3.743
6-31G(+pd+sp)	4.653	8.420	5.909	3.766	4.723	8.304	5.917	3.581
6-31G(+pd+sp)$_e$	4.496	8.454	5.816	3.958	4.529	8.352	5.803	3.824
					(5.15)	(8.75)	(6.35)	(3.61)
dimethylacetylene								
6-31G(+sd+sp)$_e$	5.952	11.725	7.876	5.773	6.057	11.721	7.945	5.664
6-31G(+pd+sp)$_e$	6.143	11.763	8.016	5.620	6.254	11.790	8.099	5.536
					(6.44)	(11.68)	(8.19)	(5.24)

[a] Basis sets with subscript 'e' have the d exponent on the heavy atom changed from 0.175 to 0.25. Present experimental values are given in parentheses for comparison.

carbon triple bond. The effect of the p function is also evident in the methylacetylene calculations.

For dimethylacetylene, the presence of the less diffuse d function, in combination with the p function, results in larger $\alpha_\perp$ and $\alpha_\parallel$ components for the 6-31G(+pd+sp)$_e$ basis set relative to the 6-31G(+sd+sp)$_e$ basis set. Furthermore, the mean polarizability increases slightly and the anisotropy decreases. The same behaviour is observable for methylacetylene using the 6-31G(+sd+sp) and 6-31G(+pd+sp) basis sets. In this case, the increase in the $\alpha_\parallel$ component is much smaller.

It is unfortunate that the basis sets required alteration for the energy to converge, but the effect of this alteration has been noted and it should not seriously affect the comparison with experiment. Table 7.6 also includes the experimental polarizabilities obtained during the present work From the table, it is evident that the MP2 mean polarizability for acetylene is too small by ≈ 3% and the polarizability anisotropy is too large by ≈ 9%. For methylacetylene, the mean polarizability is smaller by 7–10% for the basis sets used, but the polarizability anisotropy is smaller or larger, depending on the basis set chosen. For dimethylacetylene, the mean polarizability is smaller by 1–3%, and the anisotropy is larger by 5–7%. Overall, the $\alpha_\perp$ components are too small and the $\alpha_\parallel$ components agree well with experiment, except for methylacetylene where it is too small.

For multiply bonded linear molecules such as acetylene, the SCF calculations (even near the Hartree-Fock limit) underestimate $\alpha_\parallel$ and $\alpha_\perp$, and the inclusion of electron correlation lowers the magnitude of the components [34]. The effect of electron correlation on $\alpha_\perp$ and $\alpha_\parallel$ for methylacetylene and dimethylacetylene is not as straightforward. For methylacetylene, $\alpha_\perp$ is generally increased while $\alpha_\parallel$ is decreased. For dimethylacetylene, the $\alpha_\perp$ component increases for both basis sets, but $\alpha_\parallel$ increases or decreases, depending on the basis set used.

Overall, the calculations are not accurate enough to eliminate without doubt many of the literature values for α and $\Delta\alpha$, but it is probable that the values of α = 7.69 and $\Delta\alpha$ = 5.01, both at 647.1 nm, given by Alms *et al.* [12] for dimethylacetylene are too

low. Greater accuracy requires much larger basis sets than the moderately sized 6-31G(+sd+sp) and 6-31G(+pd+sp) basis sets used in the present calculations.

Conclusions

The depolarization ratio for acetylene is in good agreement with the literature values. The depolarization ratios of methylacetylene and dimethylacetylene are in agreement with the values reported by Bogaard *et al.* [15], but not those of Alms *et al.* [12]. The depolarization ratios for hexafluoro-2-butyne are the first reported values for this molecule. The mean polarizabilities for acetylene, methylacetylene and dimethylacetylene determined in the present research were high compared with the literature values and were not used in the analysis. The precision of the mean polarizability for hexafluoro-2-butyne was investigated with and without exclusion of the vibrational Raman lines, and a small variation was found between the values. Simple additivity was found for the polarizability anisotropies upon progressive substitution of methyl groups into acetylene. The ab initio calculations indicated that the mean polarizability and polarizability anisotropy given by Alms *et al.* for dimethylacetylene are too low.

The polarizability anisotropies were combined with results from Cotton-Mouton effect and field-gradient birefringence experiments to deduce some magnetic properties and the quadrupole moments of acetylene, methylacetylene and dimethylacetylene. Where comparison was possible, the magnetizability anisotropies and quadrupole moments are in excellent agreement with literature values.

References

1. Coonan, M.H. and Ritchie, G.L.D., *Chem. Phys. Lett.*, **202**, 237 (1993).
2. Buckingham, A.D., Bogaard, M.P., Dunmur, D.A., Hobbs, C.P. and Orr, B.J., *Trans. Faraday Soc.*, **66**, 1548 (1970).
3. Kling, H., Geschka, H. and Hüttner, W., *Chem. Phys. Lett.*, **96**, 631 (1983).
4. Kukolich, S.G., Read, W.G., Shea, J.A. and Campbell, E.J., *J. Am. Chem. Soc.*, **105**, 6423 (1983).
5. Hartford, S.L., Allen, W.C., Norris, C.L., Pearson, E.F. and Flygare, W.H., *Chem. Phys. Lett.*, **18**, 163 (1973).
6. Watson, J.N., *"The measurement of field-gradient induced birefringence in gases"*, Ph.D. Thesis, University of New England, (1994).
7. Blanch, E.W. and Ritchie, G.L.D., unpublished results.
8. Lamb, D.W. and Ritchie, G.L.D., unpublished results.
9. Cox, J.T. and Gordy, W., *Phys Rev.*, **101**, 1298 (1956).
10. Shoemaker, R.L. and Flygare, W.H., *J. Am. Chem. Soc.*, **91**, 5417 (1969).
11. Burnham, A.K., Buxton, L.W. and Flygare, W.H., *J. Chem. Phys.*, **67**, 4990 (1977).
12. Alms, G.R., Burnham, A.K and Flygare, W.H., *J. Chem. Phys.*, **63**, 3321 (1975).
13. Baas, F. and van den Hout, K.D., *Physica*, **95**, 597 (1979).
14. Bridge, N.J. and Buckingham, A.D., *Proc. Roy. Soc. A*, **295**, 334 (1966).
15. Bogaard, M.P., Buckingham, A.D., Pierens, R.K. and White, A.H., *J. Chem. Soc., Faraday Trans. 1*, **74**, 3008 (1978).
16. Maroulis, G. and Thakkar, A.J., *J. Chem. Phys.*, **93**, 652 (1990).
17. Maroulis, G., *Chem. Phys. Lett.*, **177**, 352 (1991).
18. Jasunski, M., Rizzo, A. and Yeager, D.L., *Chem. Phys. Lett.*, **149**, 79 (1988).
19. Jameson, C.J. and Fowler, P.W., *J. Chem. Phys.*, **85**, 3432 (1986).
20. Fowler, P.W. and Diercksen, G.H.F., *Chem. Phys. Lett.*, **167**, 105 (1990).
21. Liu, S. and Dykstra, C.E., *J. Phys. Chem.*, **91**, 1749 (1987).

22. Russell, A.J. and Spackman, M.A., unpublished results.

23. Lindh, R. and Liu, B., *J. Chem. Phys.*, **94**, 4356 (1991).

24. Dymond, J.H. and Smith, E.B., *"The virial coefficients of pure gases and mixtures"*, (Oxford University Press, Oxford, 1980).

25. Pitzer, K.S., *J. Am. Chem. Soc.*, **77**, 3427 (1955).

26. Maryott, A.A. and Buckley, F., *"Table of dielectric constants and electric dipole moments of substances in the gaseous state."*, (National Bureau of Standards, Washington, 1953).

27. Kumar, A. and Meath, W.J., *Mol. Phys.*, **75**, 311 (1992).

28. Weast, R.C., *"CRC Handbook of Chemistry and Physics"*, 70th Edition (CRC Press, Boca Raton, 1990).

29. Bishop, D.M. and Cheung, L.M., *J. Phys. Chem.*, **11**, 119 (1982).

30. Craven, I.E., Hesling, M.R. Laver, D.R., Lukins, P.B., Ritchie, G.L.D. and Vrbancich, J., *J. Chem. Phys.*, **93**, 627 (1989).

31. Coonan, M.H. and Ritchie, G.L.D., *J. Phys. Chem.*, **95**, 1220 (1991).

32. Dagg, I.R., Anderson, A., Smith, W., Missio, M., Joslin, C.G. and Read, L.A.A., *Can. J. Phys.*, **66**, 453 (1988).

33. Dykstra, C.E., Liu, S.Y. and Malik, D.J., *Adv. Chem. Phys.*, **75**, 37 (1989).

34. Spackman, M.A., *J. Phys. Chem.*, **93**, 7594 (1989).

35. Le Guennec, M., Demaison J., Wlodarczak, G. and Marsden, C.J., *J. Mol. Spectrosc.*, **160**, 471 (1993).

36. Landolt-Börnstein, *"Numerical data and functional relationships in science and technology"*, Volume II/7 (Springer-Verlag, Berlin, 1976).

37. Legon, A.C., Lister, D.G. and Rego, C.A., *Chem. Phys. Lett.*, **189**, 221 (1982).

38. Nakagawa, J., Hayashi, M., Endo, Y., Saito, S. and Hirota, E., *J. Chem. Phys.*, **80**, 5922 (1984).

39. Cederberg, J.W., Anderson, C.H. and Ramsey, N.F., *Phys. Rev.*, **136**, A960 (1964).

Chapter Eight

Pyridine, pyridazine, pyrimidine, pyrazine and *s*-triazine

Introduction

The electric and magnetic properties of the nitrogen substituted analogues of benzene have been of great interest [1-4], but the free-molecule polarizabilities of these species are poorly defined. It was the aim of the present research to determine the depolarization ratios and polarizability anisotropies (or $|3\alpha\kappa|$ values) of pyridine, pyridazine, pyrimidine, pyrazine, and *s*-triazine. The computational aim was to report systematic, electron correlated calculations of the polarizability components to gain an understanding of the change in the polarizabilities as a function of nitrogen substitution into the benzene ring. The influence of the position of two or more nitrogen atoms in the ring was also of interest. Finally, the research was stimulated by the challenge of obtaining depolarization ratios for molecules with very low vapour pressures at normal temperatures. The nitrogen analogues of interest in this study are shown in Figure 8.1.

Experimental research on the electric and magnetic properties of the diazines has been limited to solution-phase Kerr and Cotton-Mouton effect studies [4]. Kerr [5], Cotton-Mouton [6,7] and first- and second-order Zeeman effect [8] studies have been reported for pyridine. Pyridine and *s*-triazine have been studied with a previous version of the present apparatus [9], and pyridine has also been studied by Panachev *et al.* [10]. Solution-phase Kerr and Cotton-Mouton effect measurements have been reported for *s*-triazine [11]. The vibrational spectra have been recorded [12-14], and Palmer *et al.* have

investigated the electronic structures of these species using computational and experimental (particularly VUV and energy-loss spectroscopy) methods [15-17], but oscillator-strengths were not calculated.

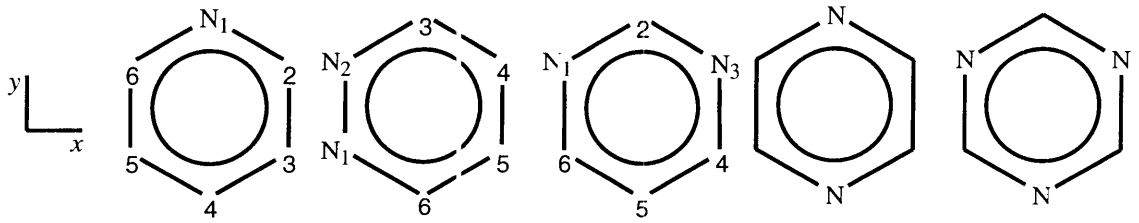

	pyridine	pyridazine	pyrimidine	pyrazine	*s*-triazine
b.p. (°C)	115	208	124	115	114
m.p. (°C)	–42	–8	21	55	86

Figure 8.1 Nitrogen analogues of benzene, including axis orientations, and melting and boiling points.

Experimental details

Pyrazine and pyrimidine (> 98%) were obtained from the Fluka Chemical Company. Pyrazine was purified by means of three sublimations, and the final purity was determined to be > 99% using high-pressure liquid-chromatography with acetonitrile and water as solvents; pyrimidine was used without further purification. Pyridazine (> 99%), obtained from the Aldrich Chemical Company, was used without further purification. Pyridine was purified using a procedure outlined in the literature [18] and the final purity was determined to be > 99.99% using gas-chromatographic analysis. The liquids were subjected to two freeze-pump-thaw cycles before use. The depolarization ratios were recorded using Version 2 of the apparatus with inclusion of the vibrational Raman lines. Integration times were 100 s for the polarized component and 200 s for the depolarized component.

The measurement of the depolarization ratios of the diazines was difficult. From Figure 8.1, it can be seen that the melting and boiling points are high relative to the operating temperature range of the apparatus (≈ 20–90 °C), which resulted in maximum

vapour pressures of approximately 10 kPa. In consequence, scattered light intensities were low and the reproducibility of the ratios was less than optimal. Typical polarized and depolarized counts for pyridine at 88 °C and 9.7 kPa were 16 400 and 345 cps, with background counts of 52 and 9 cps, respectively. Polarized and depolarized counts for pyrimidine at 90 °C and 9.1 kPa were 10 060 and 198 cps, with background counts of 9 and 3 cps, respectively. The relatively high boiling point of 208 °C for pyridazine required operating temperatures greater than had previously been attempted with the present equipment. At 120 °C and 6.9 kPa, typical polarized and depolarized counts were 1 060 and 25 cps, with background counts of 24 and 7 cps, respectively. The small depolarized component resulted in a large uncertainty in each ratio. The measurements on pyrazine were made all the more difficult by problems with dust, which were avoided by several careful sublimations, but the vapour pressure was still extremely low for this low-melting solid. Typical polarized and depolarized counts at 85 °C and 5.1 kPa were 7 600 and 173 cps, with background counts of 28 and 2 cps, respectively. The depolarization ratios are given in Table 8.1

Discussion

A summary of the depolarization ratios, mean polarizabilities and polarizability anisotropies is given in Table 8.2. The table also includes MP2/6-31G(+pd+sp) polarizabilities for 632.8 nm, experimental results for benzene from the present work and reference [19], and experimental results for *s*-triazine reported by Hesling [9]. Details of the calculated polarizabilities are given in the following section. As discussed in Chapter 5, the depolarization ratio for benzene is believed to be very reliable. For pyridine, a mean depolarization ratio of $100\rho_0 = 2.03 \pm 0.02$ was obtained. This result compares well with a previous value of $100\rho_0 = 2.05 \pm 0.04$ obtained by Hesling [9], but is in poor agreement with a value for 488.0 nm reported by Panachev *et al.* [10] of $100\rho_0 = 1.95 \pm 0.02$, although this is expected to be too small. If it is assumed that the dispersion for pyridine is the same as that for benzene, then the depolarization ratio for 632.8 nm reported by Panachev *et al.* would be $100\rho_0 \approx 1.86$, which is too low. As is noted in

Chapter 5, it is believed that the ratios for the xylenes reported by Panachev *et al.* are also too low.

Table 8.1 Depolarization ratios for pyridine, pyrazine, pyridazine and pyrimidine.

$100\rho_0$			
pyridine	pyrazine	pyridazine	pyrimidine
2.055 ± 0.013	2.259 ± 0.036	1.866 ± 0.188	1.943 ± 0.022
2.041 ± 0.014	2.284 ± 0.031	1.689 ± 0.116	2.012 ± 0.019
2.015 ± 0.014	2.238 ± 0.025	1.737 ± 0.118	1.975 ± 0.021
2.017 ± 0.014		1.753 ± 0.115	2.069 ± 0.030
2.034 ± 0.014		1.787 ± 0.114	1.992 ± 0.025
2.031 ± 0.014		1.746 ± 0.109	2.098 ± 0.025
			1.996 ± 0.025
			2.049 ± 0.025
			2.044 ± 0.029
			1.999 ± 0.029
			2.052 ± 0.029

Unfortunately, the mean polarizabilities given in Table 8.2 are from a variety of sources including Rayleigh light scattering for 632.8 nm, liquid-phase refractive indices for 589 nm and gas-phase refractive indices interpolated for 632.8 nm. Therefore, an uncertainty of ± 3% was assumed for each mean polarizability. Exceptions were made for benzene, since the mean polarizability is believed to be reliable, and for *s*-triazine, since an estimate of the uncertainty is given by Hesling.

Generally, pressures of approximately 30 kPa were necessary to determine an accurate mean polarizability with the light scattering equipment, and excellent pressure stability was required over the course of data collection. Due to the low vapour pressures available, mean polarizabilities for the diazines were not determined. A measurement of the mean polarizability of pyridine was attempted with a maximum pressure of 16 kPa,

Table 8.2 Gas-phase Rayleigh depolarization ratios, mean polarizabilities and polarizability anisotropies for benzene, pyridine, pyridazine, pyrimidine, pyrazine, and *s*-triazine.[a]

	benzene	pyridine	pyridazine	pyrimidine	pyrazine	*s*-triazine
$100\rho_0$	1.89 ± 0.01	2.03 ± 0.02	1.76 ± 0.06	2.02 ± 0.05	2.26 ± 0.03	1.91 ± 0.05[f]
α	11.56 ± 0.11[b]	10.57 ± 0.32[c]	9.78 ± 0.29[d]	9.64 ± 0.29[e]	9.99 ± 0.30[d]	8.94 ± 0.18[f]
	(12.02)	(10.79)	(9.91)	(9.85)	(10.07)	(8.02)
$\Delta\alpha$[g]	−6.23 ± 0.06	5.91 ± 0.18	5.09 ± 0.18	5.38 ± 0.18	5.91 ± 0.18	−4.85 ± 0.12
	(−5.69)	(5.85)	(5.32)	(5.35)	(5.35)	(−4.27)

[a] Values in parentheses are MP2 calculations, using the 6-31G(+pd+sp) basis set, for 632.8 nm; see computational section. The literature values for benzene were discussed in Chapter 5. The literature values for pyridine are discussed in the text.

[b] Derived from gas-phase refractive indices (an uncertainty of ± 1% was assumed) [19].

[c] Derived from liquid-phase refractive indices [38] (an uncertainty of ± 3% was assumed).

[d] Derived from liquid-phase refractive indices [20] (an uncertainty of ± 3% was assumed).

[e] Value obtained from the refractive index (n_D^{20} = 1.4998 [41]), and density measurements performed during this work using an AP PAAR DMA 55 density meter giving ρ^{25} = 1.0769 g cm^{-3} (an uncertainty of ± 3% was assumed).

[f] Rayleigh light scattering data [9].

[g] For pyridine and the diazines $\Delta\alpha$ is given as $|3\alpha\kappa|$.

giving $\alpha = 10.46 \pm 0.06$, but this is $\approx 1\%$ lower than the value quoted by Mulder *et al.* [20] (derived from reference [5]). The present value is considered to be unreliable due to the small pressure range.

From Table 8.2, substituting a CH group of the benzene ring by nitrogen to form pyridine decreases the mean polarizability by $\approx 9\%$. A second substitution decreases the mean polarizability by ≈ 14–16 % with respect to benzene, depending on the diazine. A third substitution to form *s*-triazine reduces the mean polarizability by 23% relative to benzene. The $\Delta\alpha$ (or $|3\alpha\kappa|$) values also decrease as a function of nitrogen substitution, although the values for pyridine and pyrazine are similar. The behaviour of the mean polarizability and polarizability anisotropy as a function of the number of nitrogen atoms in the ring is given in Figures 8.1 and 8.2. Prudence must be exercised in the interpretation of the data since the uncertainties are large. Further discussion of nitrogen substitution is given in the following section.

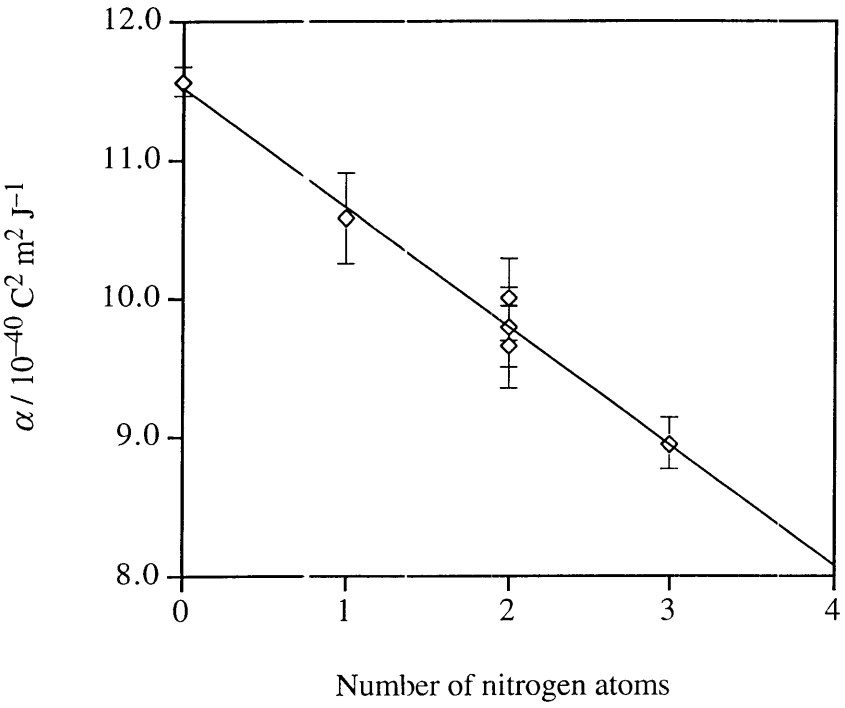

Figure 8.1 Dependence of α on the number of nitrogen atoms in the ring for molecules in the sequence benzene, pyridine, pyridazine, pyrimidine, pyrazine, and *s*-triazine.

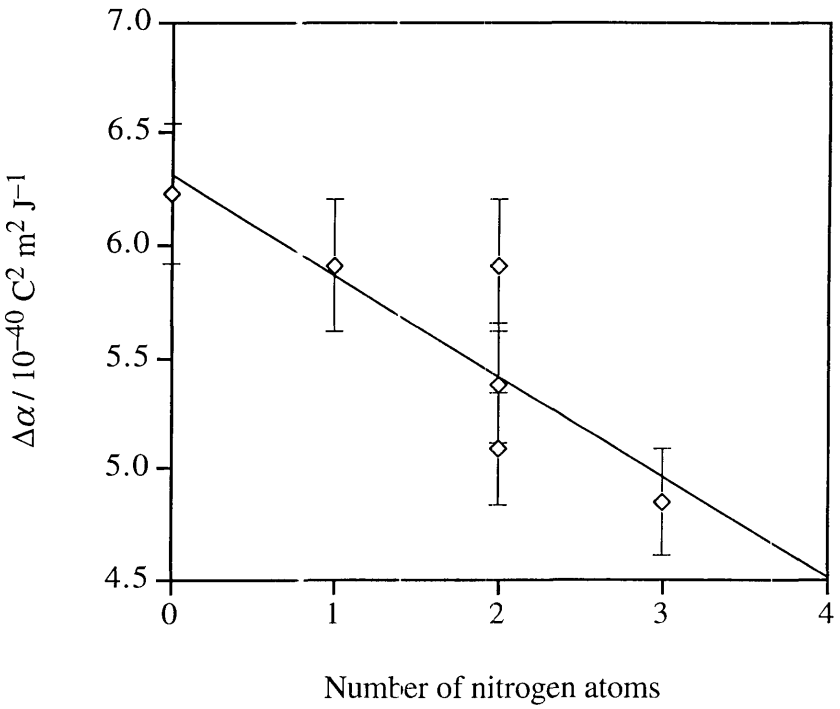

Figure 8.2 Dependence of $\Delta\alpha$ on the number of nitrogen atoms in the ring for molecules in the sequence benzene, pyridine, pyridazine, pyrimidine, pyrazine, and *s*-triazine.

Theoretical calculations

Much computational work has been done on pyridine and the diazines with varying methods and levels of theory [2,20-30]. Ab initio calculations reported by Hinchliffe and Soscún [1] on the polarizabilities of pyridine, the diazines, *s*-triazine and *s*-tetrazine are similar to the calculations reported here, but do not include electron correlation. Archibong and Thakkar [3] have calculated polarizabilities for a range of nitrogen substituted benzenes at the electron correlated level using two basis sets, one of which was the 6-31G(+sd+sp) basis set. Therefore, comparison with the present calculations will concentrate on the results of Archibong and Thakkar, and Hinchliffe and Soscún .

The aim of the present research was to calculate a set of theoretical polarizabilities which would complement the experimental data. Because of the size of the molecules, the choice of basis set was restricted to the moderately sized 6-31G(+sd+sp) and 6-

31G(+pd+sp) basis sets. The polarizabilities were calculated with the CADPAC program, and the geometries were optimized with the 6-31G** basis set. An exception was made for benzene, since an excellent neutron geometry is available [31].

Table 8.3 reports the MP2/6-31G** optimized geometries used in the calculation of the polarizabilities, and includes literature values obtained from combinations of electron-diffraction, microwave, liquid crystal NMR, infrared, and Raman methods [32-35]. From the table, it can be seen that the optimized geometries of the diazines are comparable with the experimental geometries, the main difference being the longer C–N (and for pyridazine, N–N) bond lengths. Agreement is excellent for pyridine and *s*-triazine, with only the C–H bonds being significantly shorter for the optimized geometries. Overall, the geometries are in good agreement with the literature values.

Table 8.4 reports the optical-frequency polarizabilities calculated with the 6-31G(+pd+sp) basis set. Table 8.5 reports the zero-frequency polarizabilities calculated with the 6-31G(+sd+sp) basis set and polarizabilities from recent calculations reported by Archibong and Thakkar [3], and Hinchliffe and Soscún [1]. A summary of polarizability components obtained at common laser frequencies by means of the 6-31G(+sd+sp) and 6-31G(+pd+sp) basis sets is given in Appendix I.

From Table 8.4, it can be seen that the molecules behave as normal aromatic species with the out-of-plane polarizability component, α_{zz}, being approximately half of the in-plane components of the polarizability. Substitution of a CH group by a nitrogen atom results in the less polarizable pyridine molecule, with both the mean polarizability and polarizability anisotropy decreasing. A second substitution results in a further decrease in the mean polarizability and polarizability anisotropy. The α_{zz} component is relatively unchanged within the diazines when compared with the other two components. This is easily explained since the out-of-plane contributions of the nitrogen atoms are basically independent of their positions in the ring. The mean polarizability is also relatively insensitive to the position of the second nitrogen within the benzene ring. A third nitrogen substitution to give *s*-triazine results in a further decrease in all the polarizability components. Except for *s*-triazine, the MP2/6-31G(+pd+sp) calculations

Table 8.3 Comparison of optimized and experimental geometries for pyridine, pyridazine, pyrimidine, pyrazine, and *s*-triazine.[a]

Molecule		Present work	Experiment[b]	Molecule		Present work	Experiment[b]
pyridazine	N–N	0.1347	0.1337	pyridine	N_1–C_2	0.1343	0.1344
	N–C_3	0.1342	0.1338		C_2–C_3	0.1394	0.1399
	C_3–H_7	0.1082	0.1079		C_3–C_4	0.1393	0.1398
	C_3–H_4	0.1395	0.1400		C_2–H_7	0.1083	0.1098
	C_4–C_5	0.1384	0.1385		C_3–H_8	0.1081	0.1098
	C_4–H_8	0.1081	0.1071		∠CNC	116.7	124.6
	∠NNC	118.9	119.4		$\angle C_2C_3C_4$	118.7	117.8
	∠CCC	116.9	116.9				
	∠NCH	114.5	114.9	pyrazine	N–C	0.1343	0.1337
					C–C	0.1394	0.1397
pyrimidine	C_2–H_7	0.1082	0.1082		C–H	0.1082	0.1083
	N–C_2	0.1341	0.1328		∠CNC	115.3	115.6
	N–C_4	0.1342	0.1350		∠CCH	116.8	119.9
	C_4–C_5	0.1391	0.1393				
	C_5–H_9	0.1079	0.1087	*s*-triazine	C–N	0.1338	0.1338
	C_4–H_8	0.1083	0.1079		C–H	0.1082	0.1106
	∠CCC	116.9	117.8		∠NCN	126.0	126.1
	$\angle C_5C_4H_8$	121.5	120.9				
	∠CCN	122.3	121.2				

[a] Bond lengths in nm. Atom labels correspond to the designations given in Figure 8.1.

[b] The geometries are from references [32-35].

Table 8.4 Polarizabilities at 632.8 nm for benzene, pyridine, the diazines and *s*-triazine at the SCF and MP2 levels of theory using the 6-31G(+pd+sp) basis set.[a]

	SCF					MP2				
	α_{xx}	α_{yy}	α_{zz}	α	$\Delta\alpha$	α_{xx}	α_{yy}	α_{zz}	α	$\Delta\alpha$
benzene[b]	13.56	13.56	7.48	11.53	−6.08	13.93	13.93	8.23	12.03	−5.70
pyridine	12.67	11.86	6.72	10.42	−5.59	13.10	12.37	6.92	10.80	−5.85
pyridazine	10.89	11.56	6.16	9.54	−5.10	11.40	11.96	6.38	9.91	−5.32
pyrimidine	10.82	11.20	6.03	9.35	−5.00	11.40	11.86	6.30	9.85	−5.35
pyrazine	12.31	10.43	6.08	9.61	−5.53	12.58	11.01	6.62	10.07	−5.35
s-triazine	8.72	8.72	4.83	7.42	−3.89	9.44	9.44	5.18	8.02	−4.27

[a] The sign of $\Delta\alpha$ has been assumed for pyridine and the diazines. For benzene and *s*-triazine, there are two unique components of the polarizability which permits the determination of the sign of $\Delta\alpha$.

[b] The accuracy of the calculated polarizabilities for benzene is not specifically addressed in this thesis. However, it may be noted that recent SCF calculations by Hinchliffe and Soscún [42], Augspurger and Dykstra [43] and Lazzeretti *et al.* [44,45] using moderate to large basis sets yielded results comparable to the above SCF calculations. Furthermore, the mean polarizability is in good agreement with a value obtained from dipole oscillator-strength distributions [46].

Table 8.5 A comparison of zero-frequency polarizability calculations for pyridine, pyridazine, pyrimidine, pyrazine, and *s*-triazine.

		SCF				MP2			
		α_{xx}	α_{yy}	α_{zz}	α	α_{xx}	α_{yy}	α_{zz}	α
pyridine									
	a	12.18	11.40	6.34	9.97	12.59	11.88	6.45	10.31
	b	12.06	11.31	6.63	10.00				
	c	12.47	11.61	6.34	10.14	12.89	12.08	6.45	10.48
						(12.63)	(11.87)	(6.40)	(10.30)
pyridazine									
	a	10.45	11.16	5.81	9.14	10.93	11.55	5.97	9.48
	b	10.33	11.00	6.04	9.12				
	c	10.42	11.18	5.78	9.13	10.91	11.56	5.93	9.47
						(10.78)	(11.35)	(5.89)	(9.34)
pyrimidine									
	a	10.40	10.82	5.71	8.98	10.94	11.47	5.91	9.44
	b	10.31	10.70	5.93	8.98				
	c	10.57	11.03	5.72	9.11	11.10	11.68	5.90	9.56
						(10.92)	(11.41)	(5.86)	(9.40)

Table 8.5 continued on the next page...

Table 8.5 *continued...*

pyrazine								
a	11.77	10.04	5.77	9.16	12.04	10.59	5.88	9.50
b	11.69	9.99	5.98	9.22				
c	11.87	10.04	5.74	9.22	12.15	10.58	5.85	9.53
					(11.99)	(10.41)	(5.83)	(9.41)
s-triazine								
a	8.43	8.43	4.60	7.15	9.12	9.12	4.88	7.71
b	9.26	9.26	5.25	7.92				
c	9.54	9.54	5.15	8.07	10.29	10.29	5.44	8.67
					(10.06)	(10.06)	(5.39)	(8.51)

a Present calculations using the 6-31G(+sd+sp) basis set (MP2/6-31G** optimized geometries).

b Hinchliffe and Soscún [1] using the 6-31+G(3d,3p) basis set (SCF/6-31G** optimized geometries).

c Archibong and Thakkar [3] using the 6-31G(+sd+sp) basis set (experimental geometries). Values in parentheses are SDQ-MP4 calculations.

given in Table 8.2 follow the experimentally determined trend for the mean polarizability, but are larger by up to 5%. The polarizability anisotropies are generally not as accurate and, except for pyridazine, are smaller than the experimental values.

For the literature values given in Table 8.5, Hinchliffe and Soscún used the 6-31+G(3d,3p) basis set at the SCF level with SCF/6-31G** optimized geometries, and Archibong and Thakkar used the 6-31G(+sd+sp) basis set at the SCF and MP2 levels of theory with experimental geometries. The present calculations and those of Archibong and Thakkar should differ only because of the choice of geometries. The SCF calculations of Hinchliffe and Soscún have smaller α_{xx} and α_{yy} components, and larger α_{zz} components than the present calculations, but the mean polarizabilities are comparable. The SCF and MP2 calculations of the components by Archibong and Thakkar are either slightly larger or in agreement with the present polarizability components, and this results in larger α values. The SDQ-MP4 calculations reported by Archibong and Thakkar generally reduce α and the polarizability components, although the correction is only 1–2%. As noted by Archibong and Thakkar, the inclusion of electron correlation increases the magnitude of the polarizability components.

Battaglia and Ritchie [4] have reported studies of the Kerr and Cotton-Mouton effects of pyridine and the diazines dissolved in dioxane or cyclohexane. In their analysis, it was assumed that the in-plane polarizabilities were equal ($\alpha_{xx} \approx \alpha_{yy}$). From Table 8.4, this is a reasonable assumption for pyrazine and pyrimidine, but is unsatisfactory for pyrazine. Battaglia and Ritchie determined that the polarizability anisotropies increased in the order pyridazine < pyrazine < pyrimidine, whereas the present experimental results give the order as pyridazine < pyrimidine < pyrazine. The present MP2 calculations are not accurate enough to distinguish between the polarizability anisotropies of pyrimidine and pyrazine, although the SCF values give the same order as the experimental results. The solution-phase results are also smaller than the free-molecule polarizability anisotropies, and this is a well-recognized phenomenon.

Coonan [7] has reported the principal polarizabilities for pyridine from a study of the temperature dependence of the Cotton-Mouton effect at 632.8 nm, giving α_{xx} =

13.8 ± 1.2, α_{yy} = 10.9 ± 1.6 and α_{zz} = 7.0 ± 1.0. Since Coonan used the depolarization ratio determined by Hesling [9], which is in excellent agreement with the present result, a reanalysis of the data will not alter the polarizabilities. Blanch and Ritchie [36] have reported the principal polarizabilities for pyridine from a study of the temperature dependence of the Kerr effect at 632.8 nm giving, α_{xx} = 12.83 ± 0.29, α_{yy} = 12.19 ± 0.17 and α_{zz} = 6.63 ± 0.09. The polarizabilities reported by Coonan are imprecise when compared with the values reported by Blanch and Ritchie, and the present MP2 calculations. The MP2 calculations using the 6-31G(+pd+sp) basis set are larger than the polarizabilities reported by Blanch and Ritchie, and the SCF values are in excellent agreement. This indicates that larger basis sets and higher levels of theory are required for the accurate determination of polarizabilities for large aromatic species such as pyridine.

Burnham and Gierke [37] have calculated the principal polarizabilities of pyridine from a combination of white-light single-temperature Kerr effect measurements [5], the mean polarizability [38] and the depolarization ratio [10]. The values determined from this analysis are not expected to be accurate due to the use of data obtained at various wavelengths, and assumptions made about the contributions from the hyperpolarizabilities. The principal polarizabilities have also been determined using solution-phase Kerr effect measurements by Le Fèvre and Le Fèvre [39,40] but, for the reasons mentioned above, the reported values are inaccurate.

Conclusions

The depolarization ratios for benzene, pyridine, pyridazine, pyrimidine, and pyrazine were measured. These are the first reported ratios for pyridazine, pyrimidine and pyrazine. Contributions from the vibrational Raman lines were ignored since the ratios are large. The ratios for benzene and pyridine are in excellent agreement with the known literature values. The effect of nitrogen substitution into the benzene ring, along the series benzene, pyridine, pyridazine, pyrimidine, pyrazine, and *s*-triazine was discussed and the experimental and theoretical trends were consistent. The calculations

were in excellent agreement with recent calculated values obtained from the literature. The polarizability anisotropies determined in this research are dependent on the quality of the mean polarizabilities which, for the diazines, are not known accurately or consistently by any one method. Experimental determinations of the polarizability components of pyridazine, pyrimidine and pyrazine await studies of the temperature dependence of the Kerr effect. However, because the vapour pressures are low at normal temperatures for these species, these measurements will pose a considerable challenge.

References

1. Hinchliffe, A. and Soscún, H.J., *J. Mol. Struct. (Theochem)*, **304**, 109 (1994).
2. Papadopoulos, M.G. and Waite, J., *J. Chem. Phys.*, **82**, 1435 (1985).
3. Archibong, E.F. and Thakkar, A.J., *Mol. Phys.*, **81**, 557 (1994).
4. Battaglia, M.R. and Ritchie, G.L.D., *J. Chem. Soc., Perkin Trans. 2*, 897 (1977).
5. Stuart, H.A. and Volkmann, H., *Z. Physik.*, **80**, 107 (1933).
6. Le Fèvre, R.J.W., Murthy, D.S.N. and Ritchie, G.L.D., *Aust. J. Chem.*, **24**, 1177 (1971).
7. Coonan, M.H., *"Temperature dependence of the Cotton-Mouton effect in gases"*, Ph.D. Thesis, University of New England, (1995).
8. Hamer, E. and Sutter, D.H., *Z. Naturforsch. A*, **31**, 265 (1976).
9. Hesling, M.R., *"Measurements of Rayleigh depolarization ratios of gases and vapours."*, Ph.D. Thesis, University of New England, (1990).
10. Panachev, F.I., Korableva, E.Y. and Shakhaparonov, M.I., *Russ. J. Phys. Chem.*, **50**, 1130 (1976).
11. Battaglia, M.R. and Ritchie, G.L.D., *Mol. Phys.*, **32**, 1481 (1976).
12. Arenas, J.F., Lopez-Navarrete, J.T., Otero, J.C. and Marcos, J.I., *J. Chem. Soc., Faraday Trans. 2*, **81**, 405 (1985).
13. Ozono, Y., Nibu, Y., Shimada, H. and Shimada, R., *Bull. Chem. Soc. Jpn*, **59**, 2997 (1986).
14. Kovner, M.A., Potapov, S.K., Rekhen, N.A. and Shevchenko, I.V., *Opt. Spektrosk.*, **29**, 523 (1970).
15. Palmer, M.H. and Walker, I.C., *Chem. Phys.*, **133**, 113 (1989).
16. Palmer, M.H., Walker, I.C., Guest, M.F. and Hopkirk, A., *Chem. Phys.*, **147**, 19 (1990).
17. Palmer, M.H. and Walker, I.C , *Chem. Phys.*, **157**, 187 (1991).
18. Perrin, D.D., Armarego, W.L.F. and Perrin, D.R., *"Purification of laboratory chemicals"*, 2nd Edition (Pergamon, Oxford, 1980).

19. Alms, G.R., Burnham, A.K. and Flygare, W.H., *J. Chem. Phys.*, **63**, 3321 (1975).

20. Mulder, F., Van Dijk, G. and Huiszoon, C., *Mol. Phys.*, **38**, 577 (1979).

21. Buma, W.J., Donckers, M.C.J.M. and Groenen, E.J.J., *J. Am. Chem. Soc.*, **114**, 9544 (1992).

22. Yang, W.H. and Schatz, G.C. *J. Chem. Phys.*, **97**, 3831 (1992).

23. Wiberg, K.B., Nakaji, D. and Breneman, C.M., *J. Am. Chem. Soc.*, **111**, 4178 (1989).

24. Case, D.A., Cook, M. and Karplus, M., *J. Chem. Phys.*, **73**, 3294 (1980).

25. Papadopoulos, M.G. and Waite, J., *J. Mol. Struct. (Theochem)*, **170**, 189 (1988).

26. Papadopoulos, M.G. and Waite, J., *J. Phys. Chem.*, **94**, 1755 (1990).

27. Marchese, F.T. and Jaffé, H.H., *Theoret. Chim. Acta (Berl.)*, **45**, 241 (1977).

28. de Brouckère, G. and Berthier G., *Mol. Phys.*, **47**, 209 (1982).

29. Knuts, S., Vahtras, O. and Ågren, H., *J. Mol. Struct. (Theochem)*, **279**, 249 (1993).

30. Basch, H., Garmer, D.R., Jasien, P.G., Krauss, M. and Stevens, W.J., *Chem. Phys. Lett.*, **163**, 514 (1989).

31. Jeffrey, G.A., Ruble, J.R., McMullan, R.K. and Pople, J.A., *Proc. Roy. Soc. A*, **414**, 47 (1987).

32. Pyckhout, W., Callaerts, I., Van Alsenoy, C., Geise, H.J., Almenningen, A. and Seip, R., *J. Mol. Struct.*, **147** 321 (1986).

33. Pyckhout, W., Horemans, N., Van Alsenoy, C., Geise, H.J. and Rankin, D.W.H., *J. Mol. Struct.*, **156**, 315 (1987).

34. Cradock, S., Liecheski, P.B., Rankin, D.W.H. and Robertson, H.E., *J. Am. Chem. Soc.*, **110**, 2758 (1988).

35. Cradock, S., Purves, C. and Rankin, D.W.H., *J. Mol. Struct.*, **220**, 193 (1990).

36. Blanch, E.W. and Ritchie, G.L.D., unpublished results.

37. Burnham, A.K. and Gierke, T D., *J. Chem. Phys.*, **73**, 4822 (1980).

38. Timmermans, J., *"Physico-chemical constants of pure organic compounds"*, (Elsevier, New York, 1950).

39. Le Fèvre, C.G., Le Fèvre, R J.W., Rao, B.P. and Smith, M.R., *J. Chem. Soc.*, 1188 (1959).

40. Le Fèvre, C.G. and Le Fèvre, R.J.W., *Rev. Pure Appl. Chem.*, **5**, 261 (1955).

41. Weast, R.C., *"CRC Handbook of Chemistry and Physics"*, 70th Edition (CRC Press, Boca Raton, 1990).

42. Hinchliffe, A. and Soscún, H.., *J. Mol. Struct. (Theochem)*, **300**, 1 (1993).

43. Augspurger, J.D. and Dykstra C.E., *Mol. Phys.*, **76**, 229 (1992).

44. Lazzeretti, P., Malagoli, M. and Zanasi, R., *Chem. Phys. Lett.*, **167**, 101 (1990).

45. Lazzeretti, P., Malagoli, M., Turci, L. and Zanasi, R., *J. Chem. Phys.*, **99**, 6027 (1993).

46. Kumar, A. and Meath, W.J., *Mol. Phys.*, **75**, 311 (1992).

Chapter Nine

Bromomethanes

Introduction

Experimental studies of the bromomethanes have been few in number because the more substituted species are liquids with relatively low vapour pressures, and they have a tendency to decompose when exposed to light. Furthermore, only a small number of computational studies of the bromomethanes have been reported, because the presence of the bromine atom dramatically increases the time and storage space required for the calculation of molecular properties. This chapter reports reliable values of the vapour-phase depolarization ratios of bromomethane, dibromomethane and tribromomethane. The polarizability anisotropies can be calculated by combining the depolarization ratios obtained in the present work with the known mean polarizabilities. A comparison of the electric properties of the halogenomethanes is given, and ab initio calculations are included to complement the experimental results.

Bromomethane has been extensively studied as a part of the series of mono-halogenated methanes. Rayleigh light scattering [1,2], Kerr effect [1,3-5] and Cotton-Mouton effect [6] measurements have been reported for bromomethane. The magnetic anisotropies have also been studied using the microwave Zeeman effect [7] and the NMR spectra of the deuterated species [8]. Gas-phase Kerr effect [5] measurements for dibromomethane, and solution-phase [9] and gas-phase Kerr effect [5] measurements for tribromomethane have been reported. Dipole moments for the bromomethanes have been measured by a number of methods [10-14].

Experimental details

The bromomethanes were obtained from the Aldrich Chemical Company. Bromomethane (> 99.5%) and tribromomethane (> 99%) were used without further purification; dibromomethane (> 99%) was purified by washing twice with concentrated sulfuric acid, once with distilled water, twice with 5% sodium hydroxide solution, and once with distilled water. The liquid was then dried over calcium chloride and distilled over phosphorus pentoxide. The purified liquid was stored in the dark over Type 4A molecular sieves. Breakdown products in the column precluded a gas-chromatographic analysis of this compound. The liquids underwent two freeze-pump-thaw cycles immediately before use.

The depolarization ratios were recorded with Version 2 of the apparatus. Typical depolarized and polarized counts for bromomethane at 25 °C and ≈ 100 kPa, with inclusion of the vibrational Raman lines, were 700 and 80 400 cps, with background counts of 8 and 32 cps, respectively. For dibromomethane, typical depolarized and polarized counts at 25 °C and ≈ 30 kPa, with inclusion of the vibrational Raman lines, were 608 and 39 100 cps, with background counts of 4 and 25 cps, respectively. Typical depolarized and polarized counts for tribromomethane at 86 °C and ≈ 3.3 kPa, with inclusion of the vibrational Raman lines, were 85 and 8 700 cps, with background counts of 6 and 29 cps, respectively. Integration times of 200 s for the depolarized component and 100 s for the polarized component were used for dibromomethane and tribromomethane, and the integration times were doubled for bromomethane. Density second virial coefficients for bromomethane were obtained from the literature [15]. The depolarization ratios for the bromomethanes obtained in the present research are given in Table 9.1.

Discussion

A summary of the depolarization ratios, mean polarizabilities and polarizability anisotropies for the bromomethanes is given in Table 9.2, and includes literature values. The vibrational Raman lines contributed ≈ 2.7% to the depolarization ratios for bromomethane and dibromomethane, which suggests that the depolarization ratios

previously reported for the fluoromethanes and chloromethanes [1,2] may also be too high. Considering that several of the ratios are much lower for the fluoromethanes and chloromethanes, it is likely that the vibrational Raman contribution will be proportionately higher. In fact, gas-phase Kerr effect and light scattering measurements on the fluoromethanes [16-18] confirm this prediction. The vibrational Raman contribution to the depolarization ratio of tribromomethane was negligible. It is probable that, due to the low pressures available for tribromomethane, the intensities of the vibrational Raman lines were too low to be discernible with the present apparatus.

Table 9.1 Depolarization ratios for bromomethane, dibromomethane and tribromomethane.

$100\rho_0$		
CH_3Br	CH_2Br_2	$CHBr_3$
0.868 ± 0.004	1.524 ± 0.006	0.914 ± 0.015
0.861 ± 0.004	1.545 ± 0.006	0.931 ± 0.016
0.867 ± 0.004	1.525 ± 0.006	0.882 ± 0.016
0.856 ± 0.004	1.527 ± 0.006	0.928 ± 0.023
0.839 ± 0.004[a]	1.521 ± 0.006	0.851 ± 0.017
0.842 ± 0.004[a]	1.529 ± 0.006	0.899 ± 0.016
0.843 ± 0.004[a]	1.513 ± 0.007[a]	0.921 ± 0.022[a]
0.837 ± 0.004[a]	1.491 ± 0.010[a]	0.943 ± 0.022[a]
	1.466 ± 0.008[a]	0.867 ± 0.030[a]
	1.486 ± 0.007[a]	0.912 ± 0.024[a]
	1.489 ± 0.007[a]	0.910 ± 0.030[a]
	1.511 ± 0.007[a]	0.929 ± 0.033[a]

[a] Vibrational Raman lines excluded.

Table 9.2 Depolarization ratios, m:an polarizabilities and polarizability anisotropies of bromomethane, dibromomethane an:l tribromomethane.

Molecule	λ(nm)	$100\rho_0$	α	$\Delta\alpha$	Reference
CH_3Br	632.8	0.863 ± 0.006			Present study
	632.8	0.840 ± 0.003[a]	6.42 ± 0.06[a]	2.22 ± 0.02	Present study
	632.8	0.865 ± 0.01	6.22 ± 0.06		[2]
	488.0	0.85 ± 0.01			[1]
	∞		6.63[c]		[19]
CH_2Br_2	632.8	1.53 ± 0.01			Present study
	632.8	1.49 ± 0.02[b]	9.59 ± 0.10[a]	4.58 ± 0.06[b]	Present study
	632.8		9.61		[20]
	632.8		9.38		[21]
$CHBr_3$	632.8	0.90 ± 0.04			Present study
	632.8	0.91 ± 0.03[b]		−4.9 ± 0.1	Present study
	632.8		13.11 ± 0.13		[20]
	632.8		13.02		[22]

[a] Vibrational Raman lines excluded.

[b] For dibromomethane, $\Delta\alpha$ is given as $|3\alpha\kappa|$.

[c] This value includes a vibrational polarizability correction of $\alpha_{vib} = 0.083$ [23].

The depolarization ratio for bromomethane of $100\rho_0 = 0.863 \pm 0.006$ is in excellent agreement with the value for 632.8 nm of $100\rho_0 = 0.865 \pm 0.01$ reported by Bogaard *et al.* [2], but disagrees with the value for 488.0 nm of $100\rho_0 = 0.85 \pm 0.01$ reported by Burnham *et al.* [1]. When extrapolated to 632.8 nm, the depolarization ratio reported by Burnham *et al.* will be too low ($100\rho_0 \approx 0.82$). There are no known literature values for dibromomethane and tribromomethane.

One mean polarizability was determined for bromomethane and dibromomethane with the vibrational Raman lines excluded. A mean polarizability was not recorded for tribromomethane due to the low vapour pressure available. The present mean polarizability for bromomethane does not agree with the literature values. Since other

mean polarizabilities recorded in this research have been larger than the values obtained from refractive indices, the mean polarizability given by Bogaard *et al.* [2] of α = 6.22 ± 0.06 from gas-phase refractive indices was used in the calculation of the polarizability anisotropy. The present mean polarizability for dibromomethane is within 1% of the value of α = 9.61 derived from liquid-phase refractive indices interpolated for 632.8 nm [20]. Density second virial coefficients were not used in the calculation of the mean polarizability for dibromomethane. It is surprising that the value derived from gas-phase refractive indices [21] is too low. For tribromomethane, it was assumed for the calculation of the polarizability components that the value of α = 13.11 ± 0.13 (± 1% uncertainty assumed) derived from liquid-phase refractive indices [20] interpolated for 632.8 nm was the best available mean polarizability. Measurements by Karna *et al.* [22] of solution-phase refractive indices suggest that this value is approximately 1% lower, although linear additivity of the polarizabilities for the components of the solution was assumed.

The polarizability anisotropies given in Table 9.2 were derived using the depolarization ratios which excluded the vibrational Raman lines. The polarizability anisotropy for bromomethane of $\Delta\alpha$ = 2.22 ± 0.02 reported in Table 9.2 is slightly lower than the value reported by Bogaard *et al.* of $\Delta\alpha$ = 2.253 ± 0.045, due the smaller depolarization ratio. This difference has little effect on the magnetizability anisotropy reported by Coonan and Ritchie [6] of $\Delta\chi$ = (−15.1 ± 0.8) x 10^{-29} J T^{-2}. An increase of 1.4% is evident, but the magnetizability anisotropy has an uncertainty of ≈ 5%.

A comparison of the depolarization ratios, mean polarizabilities and polarizability anisotropies for the fluoromethanes, chloromethanes and bromomethanes is given in Table 9.3. The data for the fluoromethanes and chloromethanes were taken from the literature [18]. It is noted that the depolarization ratios for the chloromethanes include the vibrational Raman contribution. Comparing the methane polarizability of α = 2.899 ± 0.003 (mean of the values given in references [21,24-27]) with the fluoromethane polarizability of α = 2.90 ± 0.03 indicates that the fluorine atom has a small polarizability similar to that of hydrogen. A consequence of the small atomic

polarizability for fluorine is small polarizability anisotropies for the fluoromethanes. The mean polarizabilities increase linear y with the number of halogen substituents within the individual halogen series, and this is shown in Figure 9.1. The increments are approximately 0.1, 2.2 and 3.3 for the fluoro-, chloro- and bromomethanes, respectively. Substitution of the larger halogens into methane results, as expected, in larger polarizability anisotropies. Figure 9.2 shows that the polarizability anisotropy is not a linear function of the number of halogen atoms.

Table 9.3 Comparison of the depolarization ratios, mean polarizabilities and polarizability anisotropies of the halogenated methanes.[a]

X	CH_3X	CH_2X_2	CHX_3
		$100\rho_0$	
F[b]	0.052 ± 0.003	0.057 ± 0.005	0.025 ± 0.002
Cl[b]	0.76 ± 0.03	1.10 ± 0.03	0.65 ± 0.03
Br[c]	0.840 ± 0.003	1.49 ± 0.02	0.91 ± 0.03
		α	
F[b]	2.90 ± 0.04	3.04 ± 0.06	3.12 ± 0.04
Cl[b]	5.06 ± 0.06	7.34 ± 0.22	9.46 ± 0.11[d]
Br[c]	6.22 ± 0.06	9.59 ± 0.10	13.11 ± 0.13[d]
		$\Delta\alpha$	
F[b]	0.25 ± 0.01	0.28 ± 0.02	−0.19 ± 0.01
Cl[b]	1.71 ± 0.04	3.00 ± 0.10	−2.97 ± 0.08
Br[c]	2.22 ± 0.02	4.58 ± 0.06	−4.9 ± 0.1

[a] All values are for 632.8 nm.

[b] From reference [18].

[c] Present research.

[d] The above values from gas-phase refractive indices agree well with the solution-phase results from Karna *et al.* [22] of α = 9.43 and 13.02 for $CHCl_3$ and $CHBr_3$.

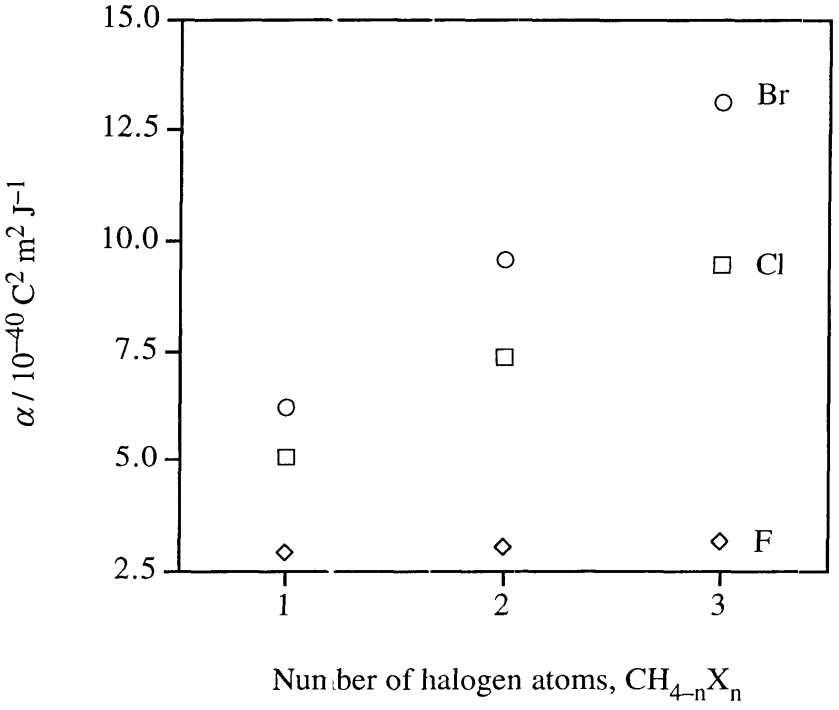

Figure 9.1 Dependence of α on the number of halogen atoms for molecules in the series fluoromethane, difluoromethane, trifluoromethane; chloromethane, dichloromethane, trichloromethane; and bromomethane, dibromomethane, tribromomethane.

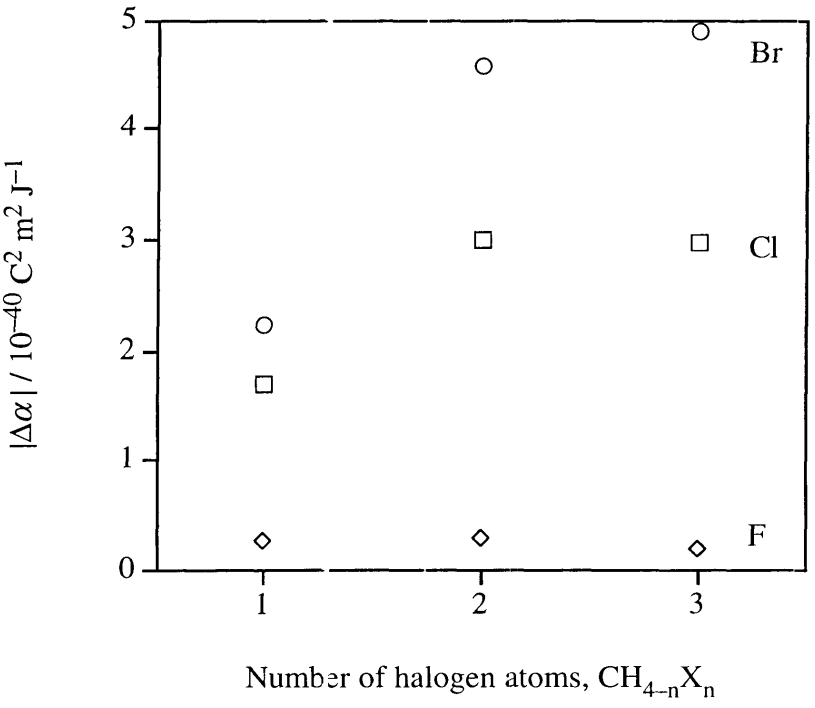

Figure 9.2 Dependence of $|\Delta\alpha|$ on the number of halogen atoms for molecules in the series fluoromethane, difluoromethane, trifluoromethane; chloromethane, dichloromethane, trichloromethane; and bromomethane, dibromomethane, tribromomethane.

Theoretical calculations

There have been few reported computational studies of the electric properties of the halogenomethanes. Dupuis and co-workers [22,28,29] have investigated polarizabilities and hyperpolarizabilities with CHF methods for the trihalogenomethanes. The studies did not include electron correlation, and used relatively small basis sets due to the size of the bromine and iodine atoms. Chong [30] has investigated the dipole moments, polarizabilities and hyperpolarizabilities for methane and the chloromethanes using density functional theory. Spackman [31] has reported calculations of the polarizabilities of methane and the fluoromethanes up to the MP2 level of theory with the 6-31G(+sd+sp) basis set. As a complement to the experimental study, calculations were undertaken to investigate the polarizabilities for the bromomethanes.

The geometries of methane and the bromomethanes were optimized with the GAMESS program using the HUZ-SV** basis set, and are given in Table 9.4. The bond length for methane is slightly shorter than the experimental r_0 geometry [32], and also differs slightly from the optimization given by Dougherty and Spackman [33] using the same basis set. This is because the core electrons are constrained in the GAMESS program whereas they are unconstrained in the CADPAC program. This effect is also present in the bromomethane optimization. For bromomethane, the r_0 geometry [32] is in excellent agreement with the optimized geometry. It is noted that r_0 structures disregard zero-point vibration.

The substitution structure [32] for dibromomethane has shorter C–H and C–Br bond lengths, and the r_0 structure [32] for tribromomethane exhibits the same effect. The optimized geometry for tribromomethane reported by Karna *et al.* for tribromomethane, using an effective core potential basis set with added polarization functions, results in comparable bond lengths of C–H = 0.1083 nm and C–Br = 0.1937 nm. The experimental C–Br bond length for tetrabromomethane reported by Allen and Sutton [34] is shorter than the optimized bond length.

The polarizabilities were calculated with the CADPAC program using the HUZ-SV(+sd+sp) basis set designed especially for calculations of this type by Dougherty and

Spackman [33]. The properties were calculated with the CHF method, except the MP2 corrections to the polarizabilities for tribromomethane and tetrabromomethane, which were calculated using the finite-field method with the GAMESS program. The zero- and optical-frequency polarizabilities are given in Tables 9.5 and 9.6. A summary of the polarizabilities for a number of common laser frequencies is given in Appendix I.

Table 9.4 Comparison of optimized and experimental geometries of methane, bromomethane, dibromomethane, tribromomethane and tetrabromomethane.[a]

		Present work	Experiment[b]
CH_4	C–H	0.1089	0.1094
CH_3Br	C–Br	0.1950	0.1933
	C–H	0.1087	0.1086
	∠HCH	111.0°	111.2°
CH_2Br_2	C–Br	0.1941	0.1927
	C–H	0.1085	0.1079
	∠BrCBr	113.3°	112.7°
$CHBr_3$	C–Br	0.1940	0.1930
	C–H	0.1086	0.1068
	∠BrCBr	111.6°	110.8°
CBr_4	C–Br	0.1951	0.193

[a] Bond lengths in nm.

[b] The geometries were obtained from references [32,34].

From Table 9.5, the mean polarizabilities calculated at the SCF (MP2) level of theory increase linearly on average by a factor of approximately 3.17 (3.38) which indicates that the successive substitution of hydrogen by bromine is additive for the series methane, bromomethane, dibromomethane, tribromomethane and tetrabromomethane. This is as expected, and is supported by the experimental results. The effect of electron correlation is to increase the individual components and the mean polarizabilities

Table 9.5 SCF and MP2 polarizability components at zero-frequency for the bromomethanes using the HUZ-SV(+sd+sp) basis set.

	SCF					MP2				
	α_{xx}	α_{yy}	α_{zz}	α	$\Delta\alpha$	α_{xx}	α_{yy}	α_{zz}	α	$\Delta\alpha$
CH_4				2.603					2.714	
CH_3Br	4.901	4.901	7.320	5.707	2.419	5.264	5.264	7.501	6.010	2.237
CH_2Br_2	12.014	6.949	7.836	8.933	4.684	12.494	7.548	8.351	9.464	4.597
$CHBr_3$	13.685	13.685	9.004	12.125	−4.681	14.427	14.427	9.773	12.875	−4.654
CBr_4				15.305					16.267	

Table 9.6 SCF and MP2 polarizability components at 632.8 nm for the bromomethanes using the HUZ-SV(+sd+sp) basis set.

	SCF					MP2				
	α_{xx}	α_{yy}	α_{zz}	α	$\Delta\alpha$	α_{xx}	α_{yy}	α_{zz}	α	$\Delta\alpha$
CH_4				2.647					2.758	
CH_3Br	5.000	5.000	7.506	5.835	2.507	5.363	5.363	7.687	6.138	2.324
CH_2Br_2	12.380	7.088	7.993	9.154	4.903	12.860	7.687	8.507	9.685	4.816
$CHBr_3$	14.072	14.072	9.172	12.438	−4.900	14.814	14.814	9.941	13.189	−4.873
CBr_4				15.718					16.681	

by more than 4%, but slightly reduce the polarizability anisotropies. A comparison of the effect of bromine substitution on the individual polarizability components is complicated by the differing symmetries within the series, which vary from C_{2v} to T_d. As expected, the polarizability of the bromine atom increases the α_{zz} component in bromomethane. This situation is reversed in tribromomethane where the α_{zz} component is smaller since it is in the direction of the C–H bond. This is reflected in the opposite signs of the polarizability anisotropies of bromomethane and tribromomethane. In dibromomethane, the z axis bisects the Br–C–Br angle and the C–Br bonds lie in the xz plane. The α_{xx} component is the largest because the bond angle is 113° and, therefore, the bromine atoms contribute a greater fraction of their polarizability to the x direction. In all cases, the α_{zz} component is in the direction of the dipole moment.

A summary of known values of the polarizability components for the bromomethanes is given in Table 9.7. The MP2 calculated polarizabilities for bromomethane are smaller than the present experimental results. The values derived for 589.3 nm from a single-temperature measurement of the Kerr effect reported by Stuart and Volkmann [4] are in excellent agreement with the present values. Similar measurements by Burnham *et al.* [1] are larger, but this is due to dispersion. As expected, the values derived from solution-phase measurements of the Kerr effect reported by Le Fèvre and Le Fèvre [3] are not as accurate due to local-field and dispersion effects. The polarizabilities for dibromomethane calculated at the MP2 level of theory are in excellent agreement with values derived from a study of the temperature dependence of the Kerr effect [5]. In this case, the calculated α_{yy} component is smaller and the other components are larger

The polarizabilities for tribromomethane calculated at the MP2 level of theory are in excellent agreement with the present experimental results. The values reported by Le Fèvre and Ritchie [9] from solution-phase measurements of the Kerr effect are in poor agreement with the present experimental values, and this is again probably due to local-field effects. The ab initio values for 694.3 nm calculated by Karna and Dupuis [29] are not as reliable as the MP2 calculated polarizabilities. The inclusion of electron correlation

Table 9.7 A comparison of the polarizability components for bromomethane, dibromomethane and tribromomethane.

Molecule	Method	λ (nm)	α_{xx}	α_{yy}	α_{zz}	Reference
CH_3Br	Rayleigh light scattering	632.8	5.48 ± 0.06	5.48 ± 0.06	7.70 ± 0.06	Present work
	Gas-phase refractive indices and single-temperature gas-phase Kerr effect	589.3	5.52	5.52	7.69	[4]
	Gas-phase refractive indices and single-temperature gas-phase Kerr effect	488.0	5.59	5.59	7.86	[1]
	Gas-phase refractive indices and solution-phase Kerr effect	589.3	5.66	5.66	7.41	[3]
	MP2 HUZI-SV(+sd+sp) polarizabilities	632.8	5.363	5.363	7.687	Present work
CH_2Br_2	Temperature dependence of the vapour-phase Kerr effect	632.8	12.64 ± 0.14	7.73 ± 0.18	8.45 ± 0.11	[5]
	MP2 HUZI-SV(+sd+sp) polarizabilities	632.8	12.860	7.687	8.507	Present work
$CHBr_3$	Rayleigh light scattering	632.8	14.73 ± 0.14	14.73 ± 0.14	9.86 ± 0.16	Present work
	Liquid-phase refractive indices and solution-phase Kerr effect	589.3	14.46	14.46	10.60	[9]
	MP2 HUZI-SV(+sd+sp) polarizabilities	632.8	14.814	14.814	9.941	Present work
	SCF polarizabilities	694.3	14.40	14.40	8.58	[29]

would increase these values, as shown by the difference between the SCF and MP2 polarizabilities in the present calculations. Karna and Dupuis acknowledged that the basis set used in their calculations was only accurate to ≈ 12–20%. Overall, the experimental polarizabilities are reproduced satisfactorily by the present calculations.

Conclusions

The depolarization ratios for bromomethane, dibromomethane and tribromomethane were measured. These are the first reported values for dibromomethane and tribromomethane. The ratios were recorded with inclusion and exclusion of the vibrational Raman lines. Mean polarizabilities were also measured for bromomethane and dibromomethane; however, the mean polarizability for bromomethane was found to be in poor agreement with a value derived from refractive indices. Polarizability anisotropies and where possible, polarizability components, were determined for the bromomethanes. The ab initio calculations were in excellent agreement with the experimental results.

References

1. Burnham, A.K., Buxton, L.W. and Flygare, W.H., *J. Chem. Phys.*, **67**, 4990 (1977).
2. Bogaard, M.P., Buckingham, A.D., Pierens, R.K. and White, A.H., *J. Chem. Soc., Faraday Trans. 1*, **74**, 3008 (1978).
3. Le Fèvre, C.G. and Le Fèvre, R.J.W., *Rev. Pure Appl. Chem.*, **5**, 261 (1955).
4. Stuart, H.A. and Volkmann, H. *Ann. Phys.*, **18**, 121 (1933).
5. Blanch, E.W. and Ritchie, G.L.D., unpublished results.
6. Coonan, M.H. and Ritchie, G.L.D., *J. Phys. Chem.*, **95**, 1220 (1991).
7. Vanderhart, D.L. and Flygare, W.H., *Mol. Phys.*, **18**, 77 (1970).
8. Van Zijl, P.C.M. and Bothner-By, A.A., *J. Magn. Res.*, **79**, 439 (1988).
9. Le Fèvre, R.J.W. and Ritchie, G.L.D., *J. Chem. Soc.*, 4933 (1963).
10. Gadhi, J., Wlodarczak, G., Legrand, J. and Demaison, J., *Chem. Phys. Lett.*, **156**, 401 (1989).
11. Carocci, S., Minguzzi, P., Tonelli, M. and Dilieto, A., *J. Mol. Spectrosc.*, **160**, 359 (1993).
12. Buckingham, A.D. and Le Fèvre, R.J.W., *J. Chem. Soc.*, **4**, 3432 (1953).
13. Lindfors, K.R. and Cornwell, C.D., *J. Chem. Phys.*, **42**, 149 (1965).
14. Schulman, R.G., Dailey, B.P. and Townes, C.H., *Phys. Rev.*, **78**, 145 (1950).
15. Dymond, J.H. and Smith, E.B., *"The virial coefficients of pure gases and mixtures"*, (Oxford University Press, Oxford, 1980).
16. Buckingham, A.D. and Orr, B.J., *Trans. Faraday Soc.*, **65**, 673 (1969).
17. Orr, B.J., Hyperpolarizabilities of halogenated methane molecules. A critical survey. In *"Nonlinear behaviour of molecules, atoms and ions in electric, magnetic and electromagnetic fields. (Proceedings of conference at Fontevraud, France in September, 1978)"*, Néel, L. (Ed.), (Elsevier, Amsterdam, 1978).
18. Miller, C.K., Orr, B.J. and Ward, J.F., *J. Chem. Phys.*, **74**, 4858 (1981).

19. Maryott, A.A. and Buckley, F, *"Table of dielectric constants and electric dipole moments of substances in the gaseous state."*, (National Bureau of Standards, Washington, 1953).

20. Vogel, A.I., *J. Chem. Soc.*, 1833 (1948).

21. Landolt-Börnstein, *"Numerical data and functional relationships in science and technology"*, Volume II/8 (Springer-Verlag, Berlin, 1962).

22. Karna, S.P., Perrin, E., Prasad, P.N. and Dupuis, M., *J. Phys. Chem.*, **95**, 4329 (1991).

23. Bishop, D.M. and Cheung, L.M., *J. Phys. Chem.*, **11**, 119 (1982).

24. Thomas, G.F. and Meath, W.J , *Mol. Phys.*, **34**, 113 (1977).

25. Hohm, U. and Kerl, K., *Mol. Phys.*, **69**, 803 (1990).

26. Hohm, U., *Mol. Phys.*, **78**, 929 (1993).

27. Hohm, U., *Mol. Phys.*, **81**, 157 (1994).

28. Karna, S.P., Dupuis, M., Perrin, E. and Prasad, P.N., *J. Chem. Phys.*, **92**, 7418 (1990).

29. Karna, S.P. and Dupuis, M., *Chem. Phys. Lett.*, **171**, 201 (1990).

30. Chong, D.P., *Chem. Phys. Lett.*, **217**, 539 (1994).

31. Spackman, M.A., *J. Phys. Chem.*, **93**, 7594 (1989).

32. Landolt-Börnstein, *"Numerical data and functional relationships in science and technology"*, Volume II/7 (Springer-Verlag, Berlin, 1976).

33. Dougherty, J. and Spackman, M.A., *Mol. Phys.*, **82**, 193 (1994).

34. Allen, P.W. and Sutton, L.E., *Acta. Cryst.*, **3**, 46 (1950).